



FINAL TECHNICAL REPORT  
1 January 1970 to 31 March 1971

David C.F. Wu and Roger C. Rudduck

AD722634

The Ohio State University  
**ElectroScience Laboratory**

Department of Electrical Engineering  
Columbus, Ohio 43212

FINAL REPORT 2969-4  
March 1971

Contract No. N00019-70-C-0252

The contractor poses no limitation or restriction on the distribution of this document by the U.S. Government to both government and non-government recipients.

Release Statement No. 2: This document has been approved for public release and sale. Its distribution is unlimited.

RELEASED TO PUBLIC PER  
SEC DEF MENO TO SEC NAV  
29 May 1969 under 6.1  
category funding program

Department of the Navy  
Naval Air Systems Command  
Washington, D.C. 20360

D D C  
RECEIVED  
MAY 11 1971  
REGISTRY  
C

Best Available Copy

DISTRIBUTION STATEMENT A  
Approved for public release  
Distribution Unlimited

91

ACCESSION NO.	
CFTI	WHITE SECTION <input checked="" type="checkbox"/>
DBC	BLUE SECTION <input type="checkbox"/>
UNANNOUNCED	<input type="checkbox"/>
JUSTIFICATION	
BY	
DISTRIBUTION/AVAILABILITY CODES	
DIST.	AVAIL. AND/OR SPECIAL
A	

## NOTICES

When Government drawings, specifications, or other data are used for any purpose other than in connection with a definitely related Government procurement operation, the United States Government thereby incurs no responsibility nor any obligation whatsoever, and the fact that the Government may have formulated, furnished, or in any way supplied the said drawings, specifications, or other data, is not to be regarded by implication or otherwise as in any manner licensing the holder or any other person or corporation, or conveying any rights or permission to manufacture, use, or sell any patented invention that may in any way be related thereto.

The Contractor poses no limitation or restriction on the distribution of this document by the U.S. Government to both government and nongovernment recipients.

This document has been approved for public release and sale. Its distribution is unlimited.

FINAL TECHNICAL REPORT  
1 January 1970 to 31 March 1971

David C.F. Wu and Roger C. Rudduck

FINAL REPORT 2969-4  
March 1971

Contract No. N00019-70-C-0252

The contractor poses no limitation or restriction on the distribution of this document by the U.S. Government to both government and non-government recipients.

Release Statement No. 2: This document has been approved for public release and sale: Its distribution is unlimited.

RELEASED TO PUBLIC PER  
SEC DEF MEMO TO SEC NAV  
29 May 1969 under 6.1  
category funding program

Department of the Navy  
Naval Air Systems Command  
Washington, D.C. 20360

## ABSTRACT

The boresight error of a practical three-dimensional antenna-radome system is analyzed by the Plane Wave Spectrum-Surface Integration technique. The Plane Wave Spectrum formulation offers a very efficient method for calculating the near field of a large circular aperture antenna. The rest of the antenna-radome analysis is carried out by using plane wave transmission coefficients through the radome and employing a surface integration technique to calculate the pattern of the antenna in the presence of the radome.

## TABLE OF CONTENTS

Chapter	Page
I. INTRODUCTION . . . . .	1
II. NEAR FIELD OF AN APERTURE ANTENNA . . . . .	6
A. Equivalence of the PWS Formulation and the Conventional Aperture Integration Method	7
B. Near Field of a Circular Aperture Antenna by the PWS Formulation	10
C. Discussions and Results	16
III. FIELDS TRANSMITTED THROUGH RADOME WALL . . . . .	22
A. Transmission and Reflection Coefficients	23
B. Transmitted Field Through a Radome Surface	29
IV. SURFACE INTEGRATION FORMULATION . . . . .	32
A. Vector Potential Formulation	32
B. Application of Surface Integration Formulation to an Ogive Radome	37
V. ANTENNA-RADOME ANALYSIS . . . . .	40
A. Near Field Calculation	41
B. Transmitted Field Through The Radome Wall	45
C. Surface Integration Analysis	47
D. Discussions and Results	50
VI. CONCLUSIONS . . . . .	54
APPENDIX A . . . . .	56
APPENDIX B . . . . .	66
APPENDIX C . . . . .	70
REFERENCES . . . . .	82

## CHAPTER I INTRODUCTION

Accurate prediction of radome boresight error has proven difficult even after years of effort by many researchers. The boresight error is defined[1] as "the angular deviation of the electrical boresight of an antenna from its reference boresight." Enclosure of an antenna by a radome can significantly change the electrical boresight such as the null direction of a conical-scanning or monopulse antenna system, or the beam-maximum direction of a highly directive antenna. Achievement of small boresight error at all look angles is a major design goal of an antenna-radome system. The boresight error of a well-designed system will be less than a few tenths of a degree. The purpose of this work is to present an accurate boresight analysis for practical three-dimensional antenna-radome systems.

The conventional two-dimensional ray-tracing technique[2] is one of the earliest existing methods for radome boresight analysis. It treats the antenna aperture distribution as a series of rays which are traced through the radome wall. A modified aperture distribution is then constructed using plane wave transmission coefficients to account for field distortions introduced by the radome. This procedure has been reversed by Tricoles[3] who considers plane waves incident on the outside of a radome and invokes reciprocity to determine boresight

errors. However, the accuracy of the ray-tracing calculations is usually uncertain due to the inherent errors associated with the ray-tracing approximations of the antenna near fields.

A two-dimensional wedge diffraction method[4] may be employed to account for the antenna near field effects on boresight calculations. This approach provides a very efficient method for calculating the antenna near field. A similar three-dimensional radome analysis formulated by Paris[5] is recently available in which the near fields of a small horn antenna are calculated by aperture integration methods. These methods give good approximations to the diffraction of the antenna fields and the transmission through the radome. However, the analysis of practical three-dimensional antenna-radome combinations has been impractical for medium and large antennas, i.e., on the order of  $75\lambda^2$  or larger. The principal difficulty encountered is the excessive computation time required for the large number of antenna near field calculations which must be made in the three-dimensional analysis.

The Plane Wave Spectrum-Surface Integration (PWS-SI) analysis that is the subject of the present study provides a method for the accurate prediction of radome boresight of a practical three-dimensional antenna-radome system. This method can be divided into the following basic steps:

(a) The near-fields of the antenna which are incident upon the radome are calculated, i.e., the fields at 2 in Fig. 1 due to the antenna at 1.

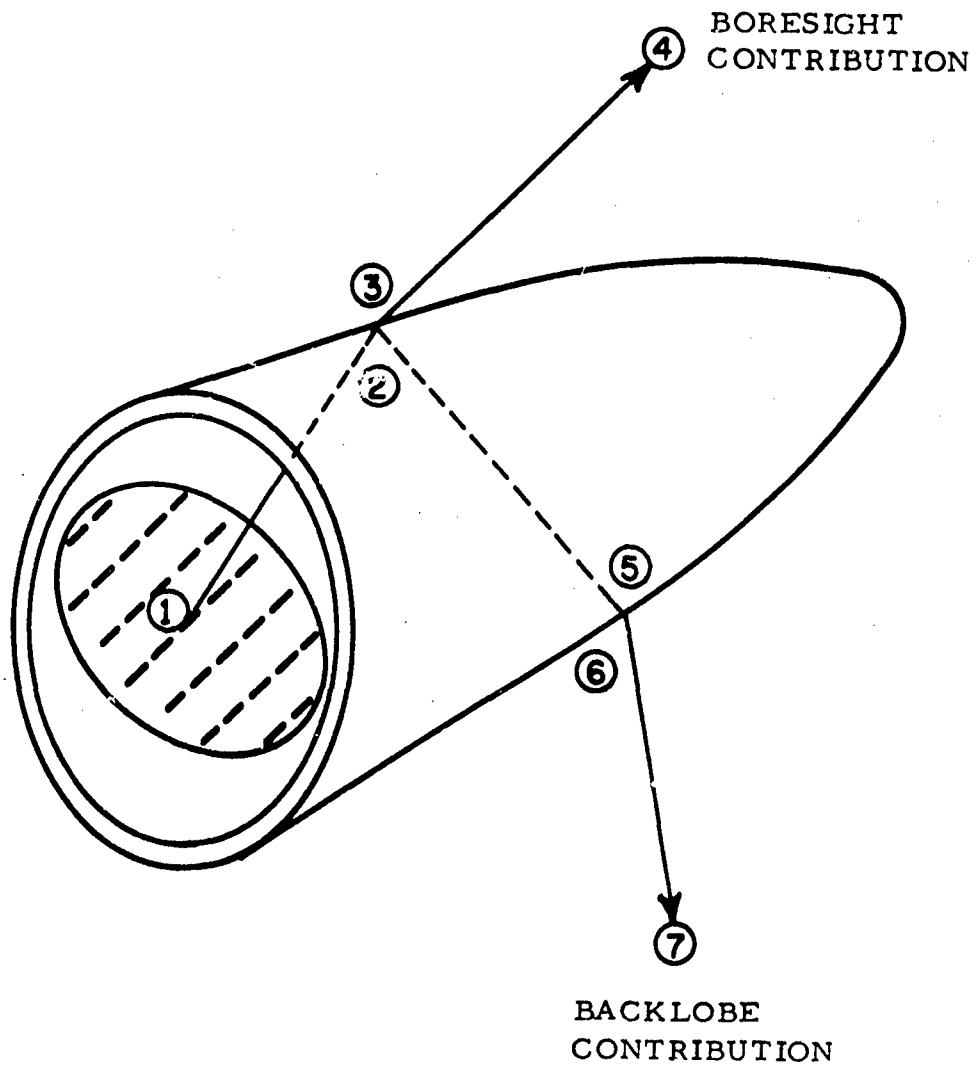


Fig. 1--3-D antenna-radome system.

(b) The transmitted fields through the radome surface are calculated, i.e., from 2 to 3 in Fig. 1.

(c) The radome boresight contribution is calculated from the transmitted fields, i.e., the radiation in region 4 is determined from the fields at 3.

In this investigation the following approximations and assumptions are adopted:

1. The near field distribution on the inner radome surface can be locally treated as a plane wave incident on a flat-dielectric sheet. The plane wave propagates in the direction of the Poynting vector. These approximations permit the use of the plane wave transmission coefficient.
2. Multiple scattering by the antenna and radome is ignored, as are scattering by any vertices and surface waves.
3. The surface integration technique considers only fields on the radome surface that lies in the antenna's forward halfspace.

In Chapter II, the plane wave spectrum solution for the near field calculations of a uniform circular aperture antenna is formulated as associated with step (a). A brief outline of the plane wave transmission coefficients for planar dielectric sheet[6] is given in Chapter III for the analysis of the transmitted field through the

radome as associated with step (b). In Chapter IV, the resulting antenna pattern is then calculated from the secondary source on the radome surface by a surface integration technique as associated with step (c). In Chapter V, the complete PWS-SI procedure is reviewed and an example boresight calculation is obtained that illustrates each step of the procedure and the results are compared with measurements.

## CHAPTER II

### NEAR FIELD OF AN APERTURE ANTENNA

In this chapter, a near field analysis for a circular aperture antenna is presented using the angular spectrum of plane waves.[7] It has been shown by Booker and Clemmow[8] that any electromagnetic field can be represented by a superposition of plane waves including inhomogeneous waves which are commonly described as surface waves. The amplitude of these waves can be determined using the Fourier integral technique if either the electric field or the magnetic field is known over the aperture plane.

The representation of the electromagnetic field as an angular spectrum of plane waves is becoming increasingly popular in the treatment of certain problems. A significant feature of this Plane Wave Spectrum (PWS) formulation is the simplicity of near field calculations for large, rotationally symmetric, circular aperture antennas. Another aspect of the PWS formulation is that it can be used to check the accuracy of the local plane wave approximation commonly employed in radome analyses which will be discussed later on.

The equivalence of the Plane Wave Spectrum (PWS) formulation and the conventional aperture integration formulation is demonstrated for an aperture antenna. Similar derivation of the equivalence of the Plane Wave Spectrum representation and of one of Rayleigh's

integral transforms demonstrated by Laior.[9] A brief outline for the near field analysis by the conventional aperture integration formulation for a uniform circular aperture is given in Appendix A.

A. Equivalence of the PWS Formulation and the Conventional Aperture Integration Method

To show the equivalence of the PWS and the conventional aperture integration formulations, we will start with the electric field expression derived from the vector potential formulation. A brief derivation of the electric field due to both the electric and the magnetic currents is presented in Chapter IV. Hence the conventional aperture integration formulation of the electric field of an aperture antenna with only the magnetic current density  $\vec{M}$  (last term of Eq. (58)) is given by

$$(1) \quad \begin{aligned} \vec{E} &= -\frac{1}{4\pi} \iint_{S_1} \nabla \times \vec{M} \left( \frac{e^{-jkr}}{r} \right) dA \\ &= -\frac{1}{4\pi} \iint_{S_1} \left( jk + \frac{1}{r} \right) \vec{M} \times \hat{r} \frac{e^{-jkr}}{r} dA. \end{aligned}$$

Where  $\hat{r}$  is the unit vector along  $r$ . The integral representation of the scalar free space Green's function is given by[9]

$$(2) \quad \frac{e^{-jkr}}{r} = \frac{1}{2\pi j} \iint_{-\infty}^{\infty} \frac{1}{k_z} e^{-j(k_x(x-x') + k_y(y-y') - k_z z)} dk_x dk_y$$

where  $k = \frac{2\pi}{\lambda} = \sqrt{k_x^2 + k_y^2 + k_z^2}$  is the free space propagation constant,  
and

$$(3) \quad \begin{aligned} k_x &= k \sin\theta \cos\phi \\ k_y &= k \sin\theta \sin\phi \\ k_z &= k \cos\theta \end{aligned}$$

As a word of caution  $k_z = \sqrt{k^2 - k_x^2 - k_y^2}$  is double-valued, and we must choose the correct root. Hence,

$$(4) \quad k_z = \begin{cases} \sqrt{k^2 - k_x^2 - k_y^2} & \text{if } k_x^2 + k_y^2 < k^2 \\ -j\sqrt{k_x^2 + k_y^2 - k^2} & \text{if } k_x^2 + k_y^2 \geq k^2 \end{cases}$$

in order to yield proper behavior of the fields at large  $|Z|$  for the time convention  $e^{+j\omega t}$ . Substituting Eq. (2) into Eq. (1), the electric field of an aperture antenna is given by

$$(5) \quad \mathbf{E} = -\frac{1}{8\pi^2 j} \iint_{S_1} \iint_{-\infty}^{\infty} \nabla \times \left[ \mathbf{M}(x', y') \frac{e^{-j(k_x(x-x') + k_y(y-y') + k_z z)}}{k_z} \right] dk_x dk_y dx' dy'$$

Since the operator  $\nabla$  is only a function of the unprime coordinate system, i.e.,  $(x, y, z)$ , Eq. (5) is reduced to

$$(5) \quad E(x, y, z) = \frac{1}{8\pi^2} \iint_{S_1} \int_{-\infty}^{\infty} \frac{1}{k_z} e^{-j(k_x(x-x') + k_y(y-y') + k_z z)} \bar{k} \times \bar{M}(x', y') dk_x dk_y dx' dy'$$

where the vector  $\bar{k}$  is given by

$$(7) \quad \bar{k} = \hat{x} k_x + \hat{y} k_y + \hat{z} k_z$$

The equivalent magnetic current density for the field of an aperture in an infinite ground plane can be expressed in terms of the aperture electric field as

$$(8) \quad \bar{M}(x', y') = 2 \bar{E} \times \hat{n}$$

where the unit normal vector  $\hat{n}$  in this case is the unit vector  $\hat{z}$ . The factor 2 in Eq. (8) results from the use of image theory with the equivalence principle.[10] For a y-polarized aperture electric field (i.e., in the case the magnetic current density is x-polarized), the electric field of Eq. (6) can be simplified to

$$(9) \quad E(x,y,z) = \frac{1}{4\pi^2} \iiint_{-\infty}^{\infty} \frac{1}{k_z} e^{-j(k_x x + k_y y + k_z z)} (\hat{y} k_z - \hat{z} k_y) F(k_x, k_y) dk_x dk_y.$$

Where  $F(k_x, k_y)$ , the angular spectrum of plane waves, is the Fourier transform of the aperture electric field  $E_y(x', y')$ , given by

$$(10) \quad F(k_x, k_y) = \iint_{S_1} E_y(x', y') e^{+j(k_x x' + k_y y')} dx' dy'.$$

Equation (9) is the PWS formulation for the fields of an aperture distribution  $E_y$ . Thus the equivalence of the Plane Wave Spectrum (PWS) formulation and the conventional aperture integration formulation Eq. (1) for an aperture antenna is shown.

#### B. Near-Field of a Circular Aperture Antenna by the PWS Formulation

As mentioned above, the PWS formulation facilitates near field calculation for a certain class of aperture antennas. The electric and magnetic fields of a y-polarized uniform electric aperture distribution (i.e.,  $E_y(x, y, 0) = 1$ ) as shown in Fig. 2 are derived in the following paragraphs by the PWS formulation. The equivalent aperture integration formulation for this problem is shown in Appendix A.

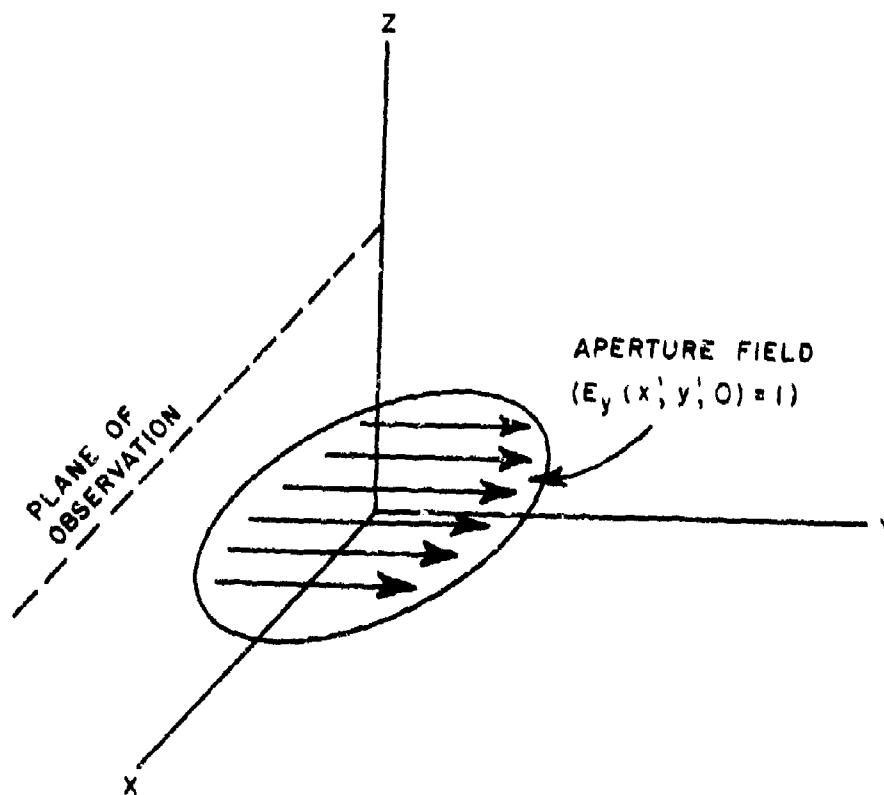


Fig. 2--Geometry of circular aperture antenna.

From Eq. (10), the angular spectrum of plane waves for a circular aperture of radius  $a$ , with uniform electric aperture distribution as shown in Fig. 2 is given by

$$\begin{aligned}
 (11) \quad F(k_x, k_y) &= \int_{-a}^a \int_{-\sqrt{a^2-y'^2}}^{\sqrt{a^2-y'^2}} e^{+j(k_x x' + k_y y')} dx' dy' \\
 &= \int_{-a}^a e^{+jk_y y'} \frac{2 \sin k_x \sqrt{a^2-y'^2}}{k_x} dy' \\
 &= \frac{4}{k_x} \int_0^a \cos k_y y' \sin k_x \sqrt{a^2-y'^2} dy' \\
 &= 2 \pi a \frac{J_1 \left( a \sqrt{k_x^2 + k_y^2} \right)}{\sqrt{k_x^2 + k_y^2}}
 \end{aligned}$$

where  $J_1$  is the Bessel function of first order. Substituting the values of  $k_x$  and  $k_y$  of Eq. (3) into Eq. (9), the radiation pattern function

$$\frac{2 \pi a J_1(ka \sin \theta)}{k \sin \theta}$$

for a circular aperture with a uniform distribution is obtained. The electric field is then obtained by substituting Eq. (11) into Eq. (9). With a change of variables

$$\begin{aligned}
 (12) \quad x &= \rho \cos \phi \\
 y &= \rho \sin \phi \\
 k_x &= k S_\rho \cos \phi' \\
 k_y &= k S_\rho \sin \phi' \\
 k_z &= k S_z = \begin{cases} k \sqrt{1-S_\rho^2} & \text{if } S_\rho < 1 \\ -jk \sqrt{S_\rho^2-1} & \text{if } S_\rho > 1 \end{cases} \\
 dk_x dk_y &= k^2 S_\rho dS_\rho d\phi'
 \end{aligned}$$

and using the identities

$$(13) \quad \int_0^{2\pi} \cos n\beta' e^{j\beta \cos(\beta'-\alpha)} d\beta' = 2\pi j^n \cos n\alpha J_n(b)$$

$$(14) \quad \int_0^{2\pi} \sin n\beta' e^{j\beta \cos(\beta'-\alpha)} d\beta' = 2\pi j^n \sin n\alpha J_n(b),$$

the  $\phi'$  integration in Eq. (9) can be analytically evaluated in terms of Bessel functions for the spectrum function  $F(k_x, k_y)$  as shown in Eq. (11). Hence, the y-component of the electric field is given by

$$\begin{aligned}
 (15) \quad E_y &= \frac{1}{\lambda^2} \int_0^\infty \int_0^{2\pi} 2\pi a \frac{J_1(ka S_\rho)}{k S_\rho} e^{-jk S_z z} \\
 &\quad e^{-jk S_\rho \rho \cos(\phi-\phi')} S_\rho dS_\rho d\phi' \\
 &= ka \int_0^\infty J_0(k S_\rho \rho) J_1(k S_\rho a) e^{-jk S_z z} dS_\rho.
 \end{aligned}$$

Employing the identity of Eq. (14) the z-component of the electric field can be obtained in a similar way giving

$$\begin{aligned}
 (16) \quad E_z &= \frac{1}{\lambda^2} \int_0^\infty \int_0^{2\pi} \frac{-S_\rho}{S_z} 2\pi a \frac{J_1(ka S_\rho)}{k S_\rho} e^{-jk S_\rho z} \\
 &\quad \sin\phi' e^{-jk S_\rho \rho \cos(\phi-\phi')} S_\rho dS_\rho d\phi' \\
 &= j \sin\phi ka \int_0^\infty \frac{S_\rho}{S_z} J_1(k S_\rho a) J_1(k S_\rho \rho) e^{-jk S_z z} dS_\rho.
 \end{aligned}$$

The corresponding expressions for the magnetic field of the uniform electric aperture field polarized in y-direction are derived using the Maxwell equations giving

$$\begin{aligned}
 (17) \quad H_x &= -\frac{Y_0}{\lambda^2} \int_0^\infty \int_0^{2\pi} 2\pi a \frac{J_1(ka S_\rho)}{k S_\rho} \frac{e^{-jk S_z z}}{S_z} \\
 &\quad (1 - S_\rho^2 \cos^2 \phi') e^{-jk S_\rho \rho \cos(\phi - \phi')} S_\rho dS_\rho d\phi' \\
 &= -Y_0 ka \int_0^\infty \frac{J_1(k S_\rho a)}{S_z} \left[ \left(1 - \frac{S_\rho^2}{2}\right) J_0(k S_\rho \rho) \right. \\
 &\quad \left. + \frac{S_\rho^2}{2} \cos 2\phi J_2(k S_\rho \rho) \right] e^{-jk S_z z} dS_\rho
 \end{aligned}$$

$$(18) \quad H_y = -\frac{Y_0 ka \sin 2\phi}{2} \int_0^\infty \frac{S_\rho^2}{S_z} J_1(k S_\rho a) J_2(k S_\rho \rho) e^{-jk S_z z} dS_\rho$$

and

$$(19) \quad H_z = -j Y_0 ka \cos \phi \int_0^\infty S_\rho J_1(k S_\rho a) J_1(k S_\rho \rho) e^{-jk S_z z} dS_\rho$$

where  $Y_0 = \sqrt{\frac{\mu}{\epsilon}}$  is the free space admittance. Hence, the electric and magnetic fields at any point in space for a circular antenna with

uniform electric aperture field polarized in  $y$ -direction are shown in Eqs. (15-19). The near field incident on the radome inner surface can thus be obtained if the radome geometry is defined.

### C. Discussions and Results

The limits of integration of Eqs. (15-19) can be restricted to the homogeneous plane wave, i.e.,  $S_p \leq 1$ , because the contribution from the inhomogeneous plane waves is insignificant at distances greater than about one wavelength from the aperture because of the exponential decay term in the integrand. Furthermore, the spectrum is concentrated at very small values of  $S_p$  for larger antennas with uniform phase distribution.

The  $y$ -component of the electric field using the PWS formulation is compared with that of the conventional aperture integration method as shown in Tables 1 to 4. Comparisons are made in the  $x$ - $z$  plane for several values of  $x$  at  $z = 2\lambda, 10\lambda, 20\lambda$  and  $40\lambda$  from the aperture antenna as shown in Fig. 2. Both the magnitude and normalized phase of the electric fields of a  $10\lambda$  diameter uniform circular aperture are also plotted as shown in Appendix A along with near fields of a two-dimensional strip antenna. Note that the electric field is symmetrical about  $x$  because of the symmetry involved in this problem. It is seen from Table 1 that the electric field using the two methods is within one percent in magnitude and about one degree in phase in the geometrical optics region (i.e.,  $-5 \leq x \leq 5$ ) even as close as  $2\lambda$  from the aperture antenna. However the agreement is not as good in the deep

null regions because numerical accuracy is hard to obtain there. Furthermore, contributions from the invisible region in the PWS formulation may not be negligible for very small values of  $z$ . For larger values of  $z$ , it is noted from Tables 2 to 4 that the maximum deviations between the two methods are within one percent in magnitude and one degree in phase.

TABLE 1  
NEAR FIELD OF A UNIFORM CIRCULAR APERTURE ANTENNA  
ON A PLANE SURFACE  $2\lambda$  FROM THE APERTURE

X	PWS FORMULATION		APERTURE INTEGRATION METHOD	
	MAGNITUDE	PHASE	MAGNITUDE	PHASE
0.0	1.3101	10.8	1.3356	11.9
0.5	0.9186	-2.6	0.9170	-2.4
1.0	1.0547	-0.2	1.0640	-0.2
1.5	0.9679	2.2	0.9670	2.0
2.0	1.0022	-3.7	0.9963	-3.9
2.5	1.0566	4.1	1.0663	4.3
3.0	0.8771	-2.1	0.8666	-2.3
3.5	1.1379	-5.2	1.1447	-5.3
4.0	1.1066	10.2	1.1083	10.3
4.5	0.8102	15.8	0.8115	16.0
5.0	0.4765	2.4	0.4751	2.3
5.5	0.2883	-40.7	0.2911	-40.8
6.0	0.1713	-116.9	0.1756	-117.6
6.5	0.1060	-215.5	0.1093	-216.7
7.0	0.0737	-332.9	0.0771	-333.6
7.5	0.0569	-467.2	0.0602	-467.0
8.0	0.0457	-613.0	0.0493	-613.1
8.5	0.0373	-768.5	0.0411	-768.0
9.0	0.0313	-928.4	0.0346	-928.9
9.5	0.0260	-1093.6	0.0293	-1093.9

TABLE 2

NEAR FIELD OF A UNIFORM CIRCULAR APERTURE ANTENNA  
ON A PLANE SURFACE  $10\lambda$  FROM THE APERTURE

X	PWS FORMULATION		APERTURE INTEGRATION METHOD	
	MAGNITUDE	PHASE	MAGNITUDE	PHASE
0.	1.0212	52.5	1.0302	53.5
0.5	0.8843	30.4	0.8873	31.1
1.0	0.9815	-11.5	0.9837	-11.6
1.5	1.0879	-19.7	1.0902	-19.9
2.0	1.1468	-1.6	1.1470	-1.6
2.5	1.2978	8.9	1.3032	8.9
3.0	1.1293	10.9	1.1308	10.7
3.5	0.8817	20.1	0.8780	20.2
4.0	0.8008	21.8	0.8011	22.0
4.5	0.6138	10.2	0.6145	10.1
5.0	0.4244	5.4	0.4234	5.5
5.5	0.3836	-6.8	0.3860	-6.7
6.0	0.3050	-38.9	0.3063	-39.4
6.5	0.1954	-66.2	0.1931	-66.5
7.0	0.1770	-89.7	0.1773	-88.8
7.5	0.1735	-141.2	0.1763	-141.0
8.0	0.1259	-203.2	0.1283	-203.9
8.5	0.8116	-251.6	0.0812	-252.8
9.0	0.0845	-301.1	0.0850	-301.0
9.5	0.0927	-380.2	0.0946	-380.1

TABLE 3

NEAR FIELD OF A UNIFORM CIRCULAR APERTURE ANTENNA  
ON A PLANE SURFACE  $20\lambda$  FROM THE APERTURE

X	PWS FORMULATION		APERTURE INTEGRATION METHOD	
	MAGNITUDE	PHASE	MAGNITUDE	PHASE
0.0	1.8419	-20.5	1.8472	-20.5
0.5	1.7179	-18.7	1.7226	-18.7
1.0	1.4222	-11.8	1.4242	-11.9
1.5	1.1528	2.7	1.1527	2.7
2.0	1.0769	19.2	1.0768	19.3
2.5	1.0960	25.9	1.0975	26.0
3.0	1.0282	22.9	1.0305	22.9
3.5	0.8355	16.2	0.8370	16.1
4.0	0.6069	13.1	0.6064	13.0
4.5	0.4757	17.3	0.4741	17.2
5.0	0.4586	14.9	0.4581	15.0
5.5	0.4346	-1.8	0.4352	-1.8
6.0	0.3497	-25.5	0.3500	-25.7
6.5	0.2380	-45.6	0.2372	-45.7
7.0	0.1773	-52.2	0.1765	-51.8
7.5	0.1897	-67.2	0.1907	-66.8
8.0	0.1983	-103.0	0.2004	-102.8
8.5	0.1694	-147.8	0.1712	-148.2
9.0	0.1160	-191.0	0.1167	-191.9
9.5	0.0758	-216.3	0.0749	-217.1

TABLE 4

NEAR FIELD OF A UNIFORM CIRCULAR APERTURE ANTENNA  
ON A PLANE SURFACE  $40\lambda$  FROM THE APERTURE

X	PWS FORMULATION		APERTURE INTEGRATION METHOD	
	MAGNITUDE	PHASE	MAGNITUDE	PHASE
0.0	1.6528	33.8	1.6536	33.9
0.5	1.6209	33.1	1.6224	33.2
1.0	1.5304	31.0	1.5315	31.0
1.5	1.3878	27.6	1.3891	27.7
2.0	1.2071	23.4	1.2080	23.4
2.5	1.0040	18.6	1.0048	18.6
3.0	0.7987	14.4	0.7992	14.4
3.5	0.6131	12.1	0.6135	12.1
4.0	0.4721	13.6	0.4721	13.5
4.5	0.3947	18.2	0.3946	18.2
5.0	0.3754	20.5	0.3754	20.5
5.5	0.3811	15.6	0.3814	15.6
6.0	0.3815	3.5	0.3820	3.5
6.5	0.3625	-13.6	0.3631	-13.6
7.0	0.3222	-33.8	0.3228	-33.9
7.5	0.2658	-55.7	0.2661	-55.9
8.0	0.2020	-76.8	0.2020	-77.1
8.5	0.1433	-93.1	0.1427	-93.4
9.0	0.1067	-99.2	0.1058	-99.3
9.5	0.1054	-102.8	0.1046	-102.4

In order to obtain numerical convergence, sixteen points per square wavelength are needed for the aperture integration method. For a  $10\lambda$  diameter aperture, i.e., about  $75\lambda^2$ , the computation time for IBM 360/75 is roughly 1 second per field point. For the PWS method, 2.5 integration points per lobe are needed to converge. The number of lobes in the PWS formulation can be determined by adding the zeros of the Bessel functions and sine and cosine functions. For example, there are about forty lobes in each of the Eqs. (15-19) for a field point  $10\lambda$  away from a  $10\lambda$  diameter aperture. The computation time for the near-field calculation is roughly 0.3 second per field point. Hence the PWS formulation results in about one third the computational time of the aperture integration method for a  $10\lambda$  diameter aperture.

For larger aperture antennas, the computation time for the near-field calculation increases proportional to  $a^2$  for the aperture integration method as compared with  $a$  for the PWS formulation where  $a$  is the radius of the circular aperture. Hence the PWS formulation is a powerful tool for calculating the near field of a large rotationally symmetric circular aperture antenna, especially if it is much larger than  $10\lambda$  diameter.

CHAPTER III  
FIELDS TRANSMITTED THROUGH RADOME WALL

In this chapter the transmitted fields at the outer radome surface are obtained. Since there is no rigorous plane wave transmission analysis for a curved dielectric layer, a curved radome surface is replaced locally by a planar sheet tangential to the point of interest as shown in Fig. 3. A brief outline is presented for the matrix formulation of the plane wave transmission and reflection coefficients for low-loss planar dielectric multilayers.[6]

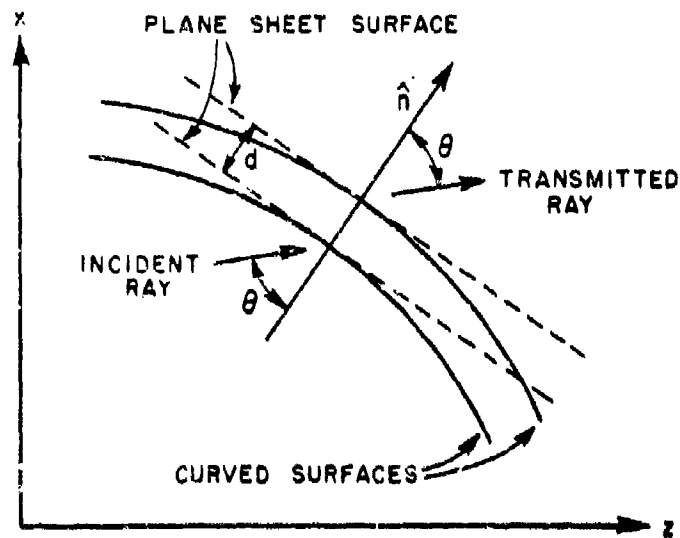


Fig. 3--Transmission through a curved dielectric.

The near field distribution on the inner radome surface is locally treated as a plane wave and is decomposed into components perpendicular and parallel to the plane of incidence. The transmitted field through the radome is then obtained by multiplying the decomposed near field by its corresponding perpendicular and parallel transmission coefficients.

The transmitted field on the radome outer surface is also obtained in terms of the Plane Wave Spectrum (PWS) formulation.[11] Since the near field of an aperture antenna can be expressed in terms of an angular spectrum of plane waves, the field transmitted through the radome can be calculated by introducing the transmission and reflection coefficients as a function of the plane wave spectra. This provides an accuracy check on the local plane wave approximation as shown in Appendix B.

A. Transmission and Reflection Coefficients

Referring to Fig. 4 the transmission and reflection coefficients are defined respectively by

$$(20) \quad T_n = \frac{F_t(p)}{F_i(Q)}$$

$$(21) \quad R = \frac{F_r(p)}{F_i(p)}$$

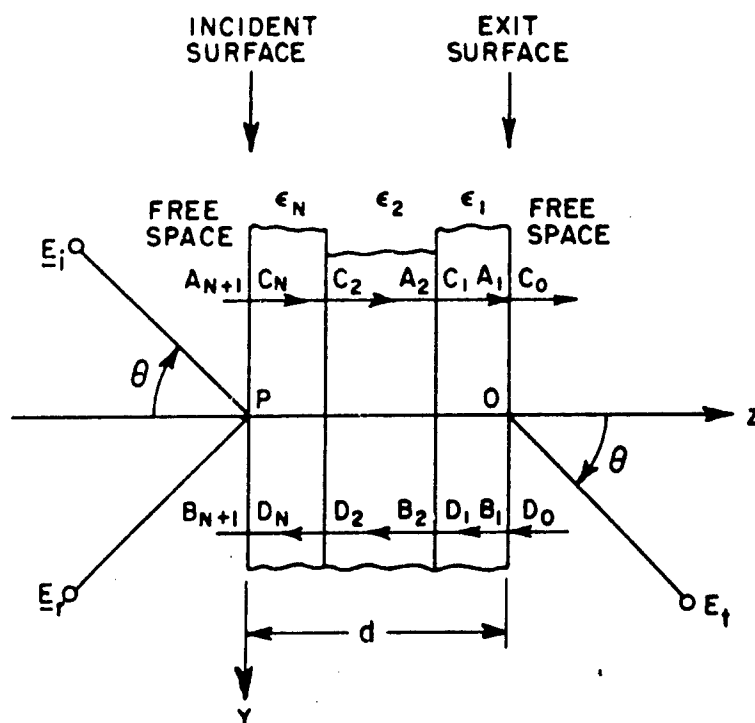


Fig. 4--Plane wave incident on plane multilayer.

where  $F$  is the electric field for perpendicular polarization and the magnetic field for parallel polarization. The subscripts  $i$ ,  $t$ ,  $r$  refer to incident, transmitted, reflected fields, respectively.

An "insertion transmission coefficient" becomes

$$(22) \quad T = \frac{F_t(Q)}{F_i(Q)} = T_n e^{jkdcos\theta}.$$

where  $d$  is the total thickness,  $\theta$  is the angle of incidence, and  $k$  is the free-space phase constant.

The resultant field in each layer consists of an outgoing plane wave and a reflected plane wave. Let the complex constants  $A_n$  and  $C_n$  represent the outgoing field intensity at the two boundaries in layer  $n$ . Similarly, let  $B_n$  and  $D_n$  represent the reflected electric field intensity. The field in an arbitrary layer, say layer  $n$ , is given by

$$(23) \quad F_x = (a e^{-\gamma_n z} + b e^{+\gamma_n z}) e^{-jky \sin \theta}.$$

By evaluating boundary conditions at the left and right boundaries of layer  $n$ , it can be shown that the matrix relationship between the constants for each layer interface becomes

$$(24) \quad \begin{pmatrix} A_n \\ B_n \end{pmatrix} = \begin{pmatrix} e^{-\gamma_n d_n} & 0 \\ 0 & e^{\gamma_n d_n} \end{pmatrix} \begin{pmatrix} C_n \\ D_n \end{pmatrix},$$

where  $d_n$  is the thickness of the layer and  $\gamma_n$  is the propagation constant. For low-loss dielectric slab, the approximations

$$(25) \quad e^{\gamma_n d_n} = e^{\alpha_n d_n} e^{j\beta d_n} \approx (1 + \alpha_n d_n) e^{j\beta_n d_n}$$

are employed where

$$(26) \quad \alpha_n \approx \frac{k \epsilon_n' \tan \alpha_n}{2 \sqrt{\epsilon_n' - \sin^2 \theta}}$$

$$(27) \quad \beta_n = k \sqrt{\epsilon_n' - \sin^2 \theta}$$

and  $\epsilon_n'$  is the relative permittivity and  $\tan \alpha_n$  is the loss tangent of layer  $n$ .

The matrix relationship between constants of different layer interfaces becomes

$$(28) \quad \begin{pmatrix} C_n \\ D_n \end{pmatrix} = \frac{1}{t_{n,n+1}} \begin{pmatrix} 1 & -r_{n+1,n} \\ -r_{n+1,n} & 1 \end{pmatrix} \begin{pmatrix} A_{n+1} \\ B_{n+1} \end{pmatrix},$$

where  $t_{n,n+1}$  denotes the interface transmission coefficient for a wave in layer  $n$  incident on the boundary of layer  $n+1$  and  $r_{n+1,n}$  denotes the interface reflection coefficient which satisfy the equations

$$(29) \quad r_{n,n+1} = -r_{n+1,n}$$

$$(30) \quad t_{n+1,n} = 1 + r_{n+1,n}$$

$$(31) \quad t_{n,n+1} = 1 + r_{n,n+1} = 1 - r_{n+1,n}$$

$$(32) \quad t_{n+1,n} t_{n,n+1} - r_{n+1,n} r_{n,n+1} = 1,$$

and the interface reflection coefficients are given by

$$(34) \quad r_{n+1,n} \approx \frac{\sqrt{\epsilon'_{n+1} - \sin^2 \theta} - \sqrt{\epsilon'_n - \sin^2 \theta}}{\sqrt{\epsilon'_{n+1} - \sin^2 \theta} + \sqrt{\epsilon'_n - \sin^2 \theta}} \quad (\text{perpendicular polarization})$$

and

$$(35) \quad r_{n+1,n} = \frac{\epsilon'_n \sqrt{\epsilon'_{n+1} - \sin^2 \theta} - \epsilon'_{n+1} \sqrt{\epsilon'_n - \sin^2 \theta}}{\epsilon'_n \sqrt{\epsilon'_{n+1} - \sin^2 \theta} + \epsilon'_{n+1} \sqrt{\epsilon'_n - \sin^2 \theta}} \quad (\text{parallel polarization})$$

Combining the two matrices gives

$$(36) \quad \begin{pmatrix} C_{n-1} \\ D_{n-1} \end{pmatrix} = \frac{1}{t_{n-1,n}} m_n \begin{pmatrix} C_n \\ D_n \end{pmatrix},$$

where

$$(37) \quad m_n = \begin{pmatrix} e^{-\gamma_n d_n} & -r_{n,n-1} e^{\gamma_n d_n} \\ -r_{n,n-1} e^{-\gamma_n d_n} & e^{\gamma_n d_n} \end{pmatrix}.$$

Repeated application of Eq. (36) for a total number of layers  $N$  relates the constants at the "incident surface" and "exit surface" as

$$(38) \quad \begin{pmatrix} C_0 \\ D_0 \end{pmatrix} = \frac{1}{t} m_1 \cdot m_2 \cdot m_3 \cdots m_N \cdot S \begin{pmatrix} A_{N+1} \\ B_{N+1} \end{pmatrix},$$

where

$$(39) \quad S = \begin{pmatrix} 1 & -r_{N+1,N} \\ -r_{N+1,N} & 1 \end{pmatrix},$$

and

$$(40) \quad t = t_{0,1} \cdot t_{1,2} \cdots t_{N,N+1}.$$

Equation (38) applies even in the general case where plane waves are incident on both outer surfaces of the multilayer, provided the two incident plane waves have the same frequency, angle of incidence, and polarization. In the situation used to define the transmission and reflection coefficients of the structure, a wave of unit amplitude is assumed to be incident on one outer surface only (say surface  $z = 0$ ), so that

$$(41) \quad A_{N+1} = 1,$$

$$(42) \quad B_{N+1} = R,$$

$$(43) \quad C_0 = T_n,$$

and

$$(44) \quad D_0 = 0.$$

Thus Eq. (38) becomes

$$(45) \quad \begin{pmatrix} T_n \\ 0 \end{pmatrix} = (1/t) M_1 \cdot M_2 \cdot M_3 \cdot M_4 \cdots M_N \cdot S \cdot \begin{pmatrix} 1 \\ R \end{pmatrix}.$$

The transmission and reflection coefficients are thus obtained using Eq. (45).

#### B. Transmitted Field Through A Radome Surface

In the transmitted field analysis of the three-dimensional antenna-radome system, the near fields on the radome inner surface obtained from Chapter II are decomposed into components perpendicular and parallel to the plane of incidence. The plane of incidence is defined by a unit normal vector  $\hat{n}$  and a unit Poynting vector  $\hat{p}$ . The unit  $\hat{n}$  which is the outward normal to the radome surface can be obtained from the radome geometry. The unit Poynting vector is obtained from the knowledge of the near fields on the radome inner surface giving

$$(46) \quad \hat{p} = \frac{\text{Re}(\vec{E} \times \vec{H}^*)}{|\text{Re}(\vec{E} \times \vec{H}^*)|}$$

where  $\text{Re}$  denotes the real part of the quantity  $(\vec{E} \times \vec{H}^*)$  and  $*$  denotes conjugate of a complex number. A unit binormal vector  $\hat{b}$  which is perpendicular to the plane of incidence can be expressed in terms of the vectors  $\hat{n}$  and  $\hat{p}$  giving

$$(47) \quad \hat{b} = \frac{\hat{n} \times \hat{p}}{|\hat{n} \times \hat{p}|}$$

A unit tangential vector  $\hat{t}$  in the plane of incidence which is tangential to the radome surface is obtained in terms of vectors  $\hat{n}$  and  $\hat{b}$  giving

$$(48) \quad \hat{t} = \hat{n} \times \hat{b}.$$

Hence the vectors  $\hat{t}$ ,  $\hat{n}$ , and  $\hat{b}$  provide a coordinate system for decomposing the incident field into perpendicular and parallel components.

It is noted that  $(\hat{b} \cdot \vec{E})\hat{b}$  is the perpendicular component of the incidence field and is also tangential to the radome surface. The part of the parallel component of the incident field which is tangential to the radome is given by  $(\hat{t} \cdot \vec{E})\hat{t}$ .

Hence the total tangential component of the transmitted electric field is given by

$$(49) \quad \vec{E}_t = [(\hat{b} \cdot \vec{E})\hat{b}] T_{\perp} + [(\hat{t} \cdot \vec{E})\hat{t}] T_{\parallel}$$

where  $T_{\perp}$  and  $T_{\parallel}$  are the transmission coefficients for perpendicular and parallel polarizations, respectively.

The corresponding expression for the tangential transmitted magnetic field  $\bar{H}_t$  is given by

$$(50) \quad \bar{H}_t = [(\hat{b} \cdot \bar{H})\hat{b}] T_{\parallel} + [(\hat{t} \cdot \bar{H})\hat{t}] T_{\perp},$$

where  $\bar{E}$  and  $\bar{H}$  in Eqs. (49) and (50) are the incident antenna near fields on the radome inner surface.

Considerable simplification is obtained by assigning the transmitted fields right on the radome inner surface instead of tracing out to the radome outer surface "rigorously." It is believed that this approximation is much more accurate than that of the local plane wave approximation and the infinite planar dielectric sheet. Equations (49) and (50) are used to obtain pattern distortions and boresight errors of a practical three-dimensional antenna-radome system.

## CHAPTER IV SURFACE INTEGRATION FORMULATION

In this chapter a surface integration technique using vector potential formulation[12] is derived that can be applied to a three-dimensional antenna-radome combination. The pattern due to the presence of the radome of an antenna-radome system is expressed in terms of the transmitted fields on the radome surface as obtained in Chapter III. The same result can be obtained from the vector formulation of the Kirchhoff-Huygens integral.[13]

### A. Vector Potential Formulation

A basic postulate in the analysis of the surface integration technique is the validity of the Huygens' equivalence principle.[10] Let  $\Sigma$  be a closed surface consisting of a radome surface  $S_1$  and an open portion of the radome  $S_2$  as shown in Fig. 5. For harmonic ( $e^{j\omega t}$ ) fields, Maxwell's equations predict that the field at every point  $(X,Y,Z)$  as shown in Fig. 5 of a linear, homogeneous, isotropic, and source-free medium bounded by  $\Sigma$  can be expressed in terms of the equivalent electric and magnetic currents  $\bar{J}_1, \bar{M}_1$  on  $S_1$  and  $\bar{J}_2, \bar{M}_2$  on  $S_2$ . We use the equivalence principle with the reservation that the currents  $\bar{J}_2, \bar{M}_2$  remain small on the open portion of the radome  $S_2$ .

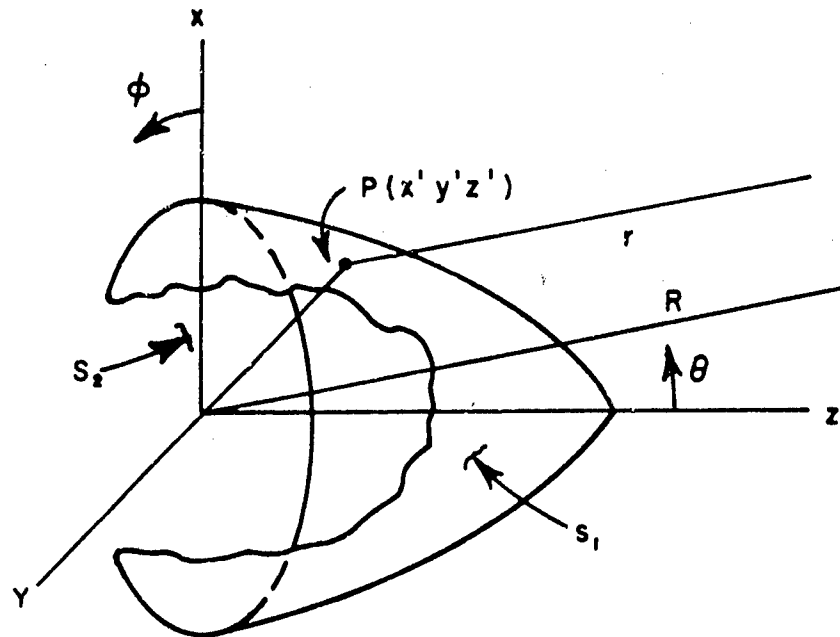


Fig. 5--Radome geometry for surface integration analysis.

Hence the electric and magnetic fields derived from the vector potential formulation can be expressed in terms of the currents  $\mathbf{J}$ ,  $\bar{\mathbf{M}}$  on surface  $S_1$  giving

$$(51) \quad \bar{\mathbf{E}} = -\frac{1}{\epsilon} \nabla \times \bar{\mathbf{F}} - \frac{\mathbf{j}}{\omega\mu\epsilon} \nabla \times \nabla \times \bar{\mathbf{A}}$$

where the potentials  $\bar{\mathbf{A}}$  and  $\bar{\mathbf{F}}$  may be written as

$$(52) \quad \bar{A} = \frac{\mu}{4\pi} \iint \bar{J} \frac{e^{-jkr}}{r} ds$$

$$(53) \quad \bar{F} = \frac{\epsilon}{4\pi} \iint \bar{M} \frac{e^{-jkr}}{r} ds.$$

A few transformations are necessary:[14]

$$(54) \quad \nabla \times \bar{J} \frac{e^{-jkr}}{r} = \frac{e^{-jkr}}{r} (\nabla \times \bar{J}) - \bar{J} \times \nabla \frac{e^{-jkr}}{r}$$

$$(55) \quad \nabla \times \bar{J} = 0.$$

Since the differentiation is with respect to observation coordinates,

$$(56) \quad \nabla \frac{e^{-jkr}}{r} = - \left( jk + \frac{1}{r} \right) \frac{e^{-jkr}}{r} \hat{r}$$

$$(57) \quad \begin{aligned} \nabla \times \left( \nabla \frac{e^{-jkr}}{r} \times \bar{J} \right) &= \nabla \frac{e^{-jkr}}{r} \nabla \cdot \bar{J} \\ &- \bar{J} \nabla \cdot \nabla \frac{e^{-jkr}}{r} + (\bar{J} \cdot \nabla) \nabla \frac{e^{-jkr}}{r} \\ &- \left( \nabla \frac{e^{-jkr}}{r} \cdot \nabla \right) \bar{J}. \end{aligned}$$

Substituting Eqs. (52) and (53) into Eq. (51) and with Eqs. (54) to (57), we have

$$(58) \quad \mathbf{E} = - \frac{j}{4\pi\omega\epsilon} \iint [(\bar{\mathbf{J}} \cdot \nabla) \nabla + k^2 \bar{\mathbf{J}} - j\omega\epsilon \bar{\mathbf{M}} \times \nabla] \frac{e^{-jkr}}{r} ds.$$

The first term of Eq. (58) can be simplified to

$$(59) \quad (\bar{\mathbf{J}} \cdot \nabla) \nabla \left( \frac{e^{-jkr}}{r} \right) = [ -k^2 (\bar{\mathbf{J}} \cdot \hat{\mathbf{r}}) \hat{\mathbf{r}} \\ + \frac{3}{r} (jk + \frac{1}{r}) (\bar{\mathbf{J}} \cdot \hat{\mathbf{r}}) \hat{\mathbf{r}} \\ - \frac{\bar{\mathbf{J}}}{r} (jk + \frac{1}{r}) ] \frac{e^{-jkr}}{r} .$$

Equation (58) is exact everywhere if the currents  $\bar{\mathbf{J}}$  and  $\bar{\mathbf{K}}$  are known over a closed surface. The magnetic field expression can be obtained using the theorem of duality as shown in Appendix A. In the case where the equivalent magnetic current is determined from image theory with the equivalence principle, as is in the case of the circular aperture antenna in Appendix A, Eq. (58) can be reduced to Eqs. (78) and (79) in Appendix A exactly by substituting Eq. (59) into Eq. (58).

Since only the far field is of interest in the surface integration formulation, only the  $r^{-1}$  terms are retained in the integrand. Hence the electric field can be expressed in terms of the currents  $\bar{\mathbf{J}}$  and  $\bar{\mathbf{M}}$  on  $S_1$  giving

$$(60) \quad \bar{E} = \frac{-j}{4\pi\omega\epsilon} \iint [ k^2 \bar{J} - k^2 (\bar{J} \cdot \hat{r}) \hat{r} - k\omega\epsilon \hat{r} \times \bar{M} ] \frac{e^{-jkr}}{r} ds.$$

The surface currents  $\bar{J}$  and  $\bar{M}$  can also be expressed in terms of the magnetic and electric fields on the surface giving

$$(61) \quad \bar{J} = \hat{n} \times \bar{H}$$

$$(62) \quad \bar{M} = \bar{E} \times \hat{n}$$

where  $\hat{n}$  is the unit normal vector on the surface  $S_1$ . Substituting Eqs. (61) and (62) into Eq. (60), the electric field in terms of  $\bar{H}$  and  $\bar{E}$  on surface  $S_1$  is obtained giving

$$(63) \quad \bar{E} = \frac{-jk}{4\pi} \iint_{S_1} \left[ \sqrt{\frac{\mu}{\epsilon}} (\hat{n} \times \bar{H}) - \left( \sqrt{\frac{\mu}{\epsilon}} (\hat{n} \times \bar{H}) \cdot \hat{r} \right) \hat{r} - \hat{r} \times (\bar{E} \times \hat{n}) \right] \frac{e^{-jkr}}{r} ds.$$

From Eq. (63), it is clear that the field  $\bar{E}(X,Y,Z)$  can be obtained with merely a knowledge of the tangential component of the fields on surface  $S_1$ . This fact is commonly employed in the analysis of microwave antennas where the E- and H-field distributions over a finite open surface located in front of the antenna are known.

B. Application of Surface Integration Formulation to an Ogive Radome

Equation (63) can be further simplified to a form most suitable for the surface integration analysis of antenna-radome combinations. Since only the far field radiation pattern is of interest, the following approximation is made:

$$(64) \quad \frac{e^{-jkr}}{r} \approx \frac{e^{-jkR}}{R} e^{+jkR(\theta')(\sin\theta \sin\theta' \cos(\phi-\phi') + \cos\theta \cos\theta')}$$

where  $R(\theta')$ , a function of  $\theta'$  related by the ogive radome geometry, is the distance from origin to the radome surface. Other variables are defined as shown in Fig. 5. Substituting the approximations for the scalar free space Green's function of Eq. (64) into Eq. (63), the far field at any point,  $(X, Y, Z)$  can be calculated.

The Y-component of the electric field in X-Z plane is derived in the following to calculate the boresight error for perpendicular polarization. The far field approximation of the unit vector  $\hat{r}$  in the X-Z plane is given by

$$(65) \quad \hat{r} = \sin\theta \hat{X} + \cos\theta \hat{Z}.$$

The contribution of the first term of Eq. (63) to the Y-component of the electric field is given by

$$(66) \quad \sqrt{\frac{\mu}{\epsilon}} (\mathbf{n} \times \overline{\mathbf{H}}_t) \Big|_Y = \sqrt{\frac{\mu}{\epsilon}} (n_Z H_{tX} - n_X H_{tZ}).$$

There is no Y-component in the second term of Eq. (63). The contribution of the last term of Eq. (63) to the Y-component of the electric field is given by

$$(67) \quad \begin{aligned} \hat{\mathbf{r}} \times (\overline{\mathbf{E}}_t \times \hat{\mathbf{n}}) \Big|_Y &= [(\hat{\mathbf{r}} \cdot \hat{\mathbf{n}}) \overline{\mathbf{E}}_t - (\hat{\mathbf{r}} \cdot \overline{\mathbf{E}}_t) \hat{\mathbf{n}}]_Y \\ &= (\sin\theta n_X + \cos\theta n_Z) E_{tY} \\ &\quad - (\sin\theta E_{tX} + \cos\theta E_{tZ}) n_Y, \end{aligned}$$

where  $n_X, n_Y, n_Z$  are the X Y Z-components of the unit normal vector  $\hat{\mathbf{n}}$ . Hence the Y-component of the electric far field is given in terms of the tangential field on the radome surface as

$$(68) \quad E_Y(0) = \frac{-jk}{4\pi} \frac{e^{-jkR}}{R} \iint [\sin\theta n_Y E_{tX} + \cos\theta n_Y E_{tZ} - \sin\theta n_X E_{tY} \\ - \cos\theta n_Z E_{tY} \\ - \sqrt{\frac{\mu}{\epsilon}} n_X H_{tZ} + \sqrt{\frac{\mu}{\epsilon}} n_Z H_{tX}] \\ e^{+jkR(\theta')} (\sin\theta \sin\theta' \cos\phi' + \cos\theta \cos\theta') ds.$$

Note that  $E_{tX}$ ,  $E_{tY}$ ,  $E_{tZ}$ ,  $H_{tX}$  and  $H_{tZ}$  are the components of the transmitted tangential electric and magnetic fields  $\bar{E}_t$  and  $\bar{H}_t$  of Eqs. (49) and (50) on the radome surface and  $\theta'$  and  $\phi'$  are the variables of integrations.

## CHAPTER V ANTENNA-RADOME ANALYSIS

The Plane Wave Spectrum-Surface Integration Method developed in Chapters II through IV is now applied to a practical three-dimensional antenna-radome combination. A description of the complete procedure for boresight calculation is presented and an example is worked out to illustrate each step in the procedure.

As pointed out in Chapter I the basic approach for analysis of the three-dimensional antenna-radome combination can be divided into three steps which are restated as follows:

1. The near fields of the antenna which are incident upon the radome are calculated.
2. The transmission through the radome is calculated.
3. The radome boresight is determined from the beam maximum of the distorted antenna pattern which in turn is calculated from the transmitted field.

Detailed explanations for the three steps are presented in the following paragraphs.



The radome geometry, as shown in Fig. 6, can be defined by a general second degree equation. For ogival shapes, the equation is

$$(69) \quad f(\rho, Z) = Z^2 + (\rho - L_2)^2 - R_1^2 = 0$$

where  $R_1$  is the radius of curvature,  $L_2$  is the distance from origin to the center of curvature as shown in Fig. 6. Thus, for a given  $Z = Z_0$  the value of  $\rho_0$  at  $Y = 0$  plane can be calculated from Eq. (69). Unit normal vectors at the radome contour are computed by

$$(70) \quad \hat{n} = \frac{\nabla f}{|\nabla f|} = n_Z \hat{Z} + n_\rho \hat{\rho}$$

where  $\nabla f$  equals the gradient of Eq. (69),

$\hat{Z}$  is unit Z vector,

$\hat{\rho}$  is unit X vector at  $Y = 0$  plane.

Now to define any point on the three-dimensional radome, the angle  $\phi$  is the angle from the X-Z plane. Hence the values of  $X_0$  and  $Y_0$  are calculated from  $\rho_0$  and  $\phi_0$  giving

$$(71) \quad X_0 = \rho_0 \cos \phi_0$$

$$(72) \quad Y_0 = \rho_0 \sin \phi_0$$

and the corresponding unit normal vector is given by

$$\begin{aligned}
 (73) \quad \hat{n} &= n_X \hat{X} + n_Y \hat{Y} + n_Z \hat{Z} \\
 &= n_\rho \cos\phi \hat{X} + n_\rho \sin\phi \hat{Y} + n_Z \hat{Z}.
 \end{aligned}$$

Since the near field expressions as derived in Chapter II are in the antenna coordinates  $(x,y,z)$ , it is necessary to obtain the points on the radome inner surface in terms of the antenna coordinates.

The aperture antenna in this case is restricted to rotate at the gimbal point along the  $Y$  axis. Hence the coordinate transformation from  $(X,Y,Z)$  to  $(x,y,z)$  systems of coordinates is given by

$$(74) \quad \begin{pmatrix} x \\ y \\ z \end{pmatrix} = \begin{pmatrix} \cos\Omega & 0 & -\sin\Omega \\ 0 & 1 & 0 \\ \sin\Omega & 0 & \cos\Omega \end{pmatrix} \begin{pmatrix} X \\ Y \\ Z \end{pmatrix} - \begin{pmatrix} 0 \\ 0 \\ L_3 \end{pmatrix}$$

where  $\Omega$  is the look angle of the aperture antenna and  $L_3$  is the distance from the aperture antenna to the gimbal point in antenna coordinates as shown in Fig. 6. The points  $(x,y,z)$  on the radome inner surface of Eq. (74) are obtained in terms of antenna coordinates. The near fields of an arbitrary planar antenna which are incident upon the radome are calculated from Eqs. (9) and (10). The antenna near field components for the present example are restated here for convenience from Eqs. (15) through (19).

$$(75) \quad E_y = Ka \int_0^1 J_0(k S_\rho \rho) J_1(k S_\rho a) e^{-jk S_z z} dS_\rho$$

$$(76) \quad E_z = j \sin \phi ka \int_0^1 \frac{S_\rho}{S_z} J_1(k S_\rho a) J_1(k S_\rho \rho) e^{-jk S_z z} dS_\rho$$

$$(77) \quad H_x = -Y_0 ka \int_0^1 \frac{J_1(k S_\rho a)}{S_z} \left[ \left( 1 - \frac{S_\rho^2}{2} \right) J_0(k S_\rho \rho) + \frac{S_\rho^2}{2} \cos 2\phi J_2(k S_\rho \rho) \right] e^{-jk S_z z} dS_\rho$$

$$(78) \quad H_y = \frac{-Y_0 ka \sin 2\phi}{2} \int_0^1 \frac{S_\rho^2}{S_z} J_1(k S_\rho a) J_2(k S_\rho \rho) e^{-jk S_z z} dS_\rho$$

and

$$(79) \quad H_z = -j Y_0 ka \cos \phi \int_0^1 S_\rho J_1(k S_\rho a) J_1(k S_\rho \rho) e^{-jk S_z z} dS_\rho,$$

where

$$(80) \quad \rho = \sqrt{x^2 + y^2}$$

and

$$(81) \quad \phi = \tan^{-1} \frac{y}{x}$$

The limits of integration of Eqs. (75) through (79) are restricted to the homogeneous plane waves, i.e.,  $S_\rho < 1$  since the contributions from the inhomogeneous plane waves, i.e.,  $S_\rho \geq 1$ , are insignificant as discussed in Chapter II.

#### B. Transmitted Field Through The Radome Wall

The transmission through the radome wall developed in Chapter III is performed in the antenna coordinates. In the transmitted field analysis, the near fields on the radome inner surface are decomposed into perpendicular and parallel components in the plane of incidence. A basis which contains vectors  $\hat{t}$ ,  $\hat{n}$ ,  $\hat{b}$  commonly known as tangential, normal, and binormal unit vectors is formulated for decomposing the incident field into the perpendicular and parallel components giving

$$(82) \quad \hat{b} = \frac{\hat{n} \times \hat{p}}{|\hat{n} \times \hat{p}|}$$

$$(83) \quad \hat{t} = \hat{n} \times \hat{b}.$$

The unit normal vector  $\hat{n}$  obtained in the radome coordinates Eq. (73) is transformed to the antenna coordinates.

The transformation for the vector components from the radome coordinates to the antenna coordinates is given by

$$(84) \quad \begin{pmatrix} A_x \\ A_y \\ A_z \end{pmatrix} = \begin{pmatrix} \cos\Omega & 0 & -\sin\Omega \\ 0 & 1 & 0 \\ \sin\Omega & 0 & \cos\Omega \end{pmatrix} \begin{pmatrix} A_X \\ A_Y \\ A_Z \end{pmatrix}$$

where  $A_x, A_y, A_z$  are the components of the vector  $\bar{A}$  in the  $(x,y,z)$  system of coordinates.

The unit Poynting vector  $\hat{p}$  is obtained from the knowledge of the near fields on the radome inner surface giving

$$(85) \quad \hat{p} = \frac{\text{Re}(\bar{E} \times \bar{H}^*)}{|\text{Re}(\bar{E} \times \bar{H}^*)|}$$

and the angle of incidence is given by

$$(86) \quad \theta = \cos^{-1} (\hat{n} \cdot \hat{p}).$$

Hence the tangential components of the transmitted electric and magnetic fields that were given in Chapter III are given again for completeness by

$$(87) \quad \bar{E}_t = [(\hat{b} \cdot \bar{E}) \hat{b}] T_{\perp} + [(\hat{t} \cdot \bar{E}) \hat{t}] T_{\parallel}$$

$$(88) \quad \bar{H}_t = [(\hat{b} \cdot \bar{H}) \hat{b}] T_{\parallel} + [(\hat{t} \cdot \bar{H}) \hat{t}] T_{\perp}.$$

Where  $T_{\perp}$  and  $T_{\parallel}$  are the transmission coefficients for perpendicular and parallel polarizations, respectively.

### C. Surface Integration Analysis

The Surface Integration Method developed in Chapter IV is now applied in order to determine pattern distortion and the corresponding boresight error. Since all of the mathematical operations are performed in the radome coordinates, it is necessary to transform to radome coordinates all of the calculated quantities which were in terms of the antenna coordinates. The transformation from the antenna coordinates to the radome coordinates is given by

$$(89) \quad \begin{pmatrix} A_X \\ A_Y \\ A_Z \end{pmatrix} = \begin{pmatrix} \cos \Omega & 0 & \sin \Omega \\ 0 & 1 & 0 \\ -\sin \Omega & 0 & \cos \Omega \end{pmatrix} \begin{pmatrix} A_x \\ A_y \\ A_z \end{pmatrix}$$

With all the calculated quantities in terms of the radome coordinates the pattern distortion can be determined by

$$\begin{aligned}
 (90) \quad E_Y = & \frac{-jk}{4\pi} \frac{e^{-jkR}}{R} \iint [-n_X(\sin\theta E_{tY} + \sqrt{\frac{\mu}{\epsilon}} H_{tZ}) \\
 & + n_Y(\sin\theta E_{tX} + \cos\theta E_{tZ}) \\
 & + n_Z(-\cos\theta E_{tY} + \sqrt{\frac{\mu}{\epsilon}} H_{tX})] e^{+jkR(\theta')(\sin\theta \sin\theta' \cos\phi' \\
 & + \cos\theta \cos\theta')} ds
 \end{aligned}$$

where  $E_{tX}$ ,  $E_{tY}$ ,  $E_{tZ}$ ,  $H_{tX}$ ,  $H_{tZ}$  are the tangential components of the transmitted field in radome coordinates.

The trapezoidal integration method is employed for Eq. (90). Equal increments are taken along the ogive surface as shown in Fig. 6 starting from the tip of the radome and integration around the rings is performed. Enough points are taken around the rings such that at least one point per wavelength square is used in the integration.

The problem of interest is to analyze the distortion introduced by the radome as a function of antenna look angle  $\Omega$ . The deviation of the electrical boresight (defined as the beam maximum) from the geometrical boresight axis at  $\Omega$  as shown in Fig. 6 is defined as the boresight error.

The boresight error of an antenna-radome system can be determined by numerous methods such as beam maximum deviation, null-shift of a monopulse difference pattern and phase distortion of a monopulse

antenna. The boresight error is evaluated in this analysis from the deviation of the beam maximum. If the antenna is scanning in a particular direction and the boresight error is in the same direction it is defined to be a positive error.

In calculating the boresight error several considerations simplify the task. The beam maximum is generally within a fraction of a degree from the look angle  $\Omega$  (boresight axis). Hence only a small portion of the pattern is necessary to determine the boresight errors. The pattern in the presence of the radome is calculated from Eq. (90). In addition, the pattern over a small interval enclosing the beam maximum is monotonically decreasing on both sides of the beam maximum and approximately symmetrical. The beam maximum is determined by computing one pattern point on each side of the antenna look angle so as to enclose the beam maximum in a bracket. By use of the symmetry and monotonic properties of the pattern the relative values of the two calculated points indicate which point is closest to the beam maximum. From this information a third pattern point is calculated which halves the size of the bracket containing the beam maximum. Examination of the field magnitudes at each end of the new bracket now predicts the calculation of a fourth pattern point which again halves the bracket containing the beam maximum. This process can be continued indefinitely to obtain the beam maximum location to any desired accuracy. Starting with a two degree interval the beam maximum will be known to within  $1/2^{n-1}$  degrees for  $n$  such calculations. In this analysis twelve such calculations are performed which gives a precision of about 0.00049 degrees or 0.0085 milliradians in the beam maximum location.

#### D. Discussions and Results

To check the validity of the surface integration formulation, free space integration is performed using Eq. (90). This is done by setting the transmission coefficients equal to unity (i.e., ideal radome) in the transmitted field expressions of Eqs. (87) and (88). This integration should faithfully yield the far field  $\left| \frac{J_1(x)}{x} \right|$  pattern. Figure 7 shows the calculated result for an ideal ogive radome with fineness ratio 1:1, as compared with  $\left| \frac{J_1(x)}{x} \right|$  pattern. It is seen from Fig. 7 that the PWS-SI analysis yields excellent agreements in the free space check.

Boresight error calculations using the three-dimensional Plane Wave Spectrum - Surface Integration (PWS-SI) analysis have been obtained for two ogive radomes with half-wavelength wall design and with fineness ratios 1:1 and 2:1 are shown in Figs. 8 and 9, respectively. The corresponding measured boresight error data shown in Figs. 8 and 9 were supplied by the U. S. Naval Air Development Center at Johnsville, Pennsylvania.[15] It is noted from Fig. 8 that there is essentially no boresight error in the nose-on region for the radome with fineness ratio 1:1. However the boresight error for the radome with 2:1 fineness ratio peaks up at look angles around 10 to 15 degrees. Considering that some experimental error may be present in the measured results, it is concluded from Fig. 8 and 9 that the PWS-SI method is a powerful technique in analyzing three-dimensional antenna-radome combinations.

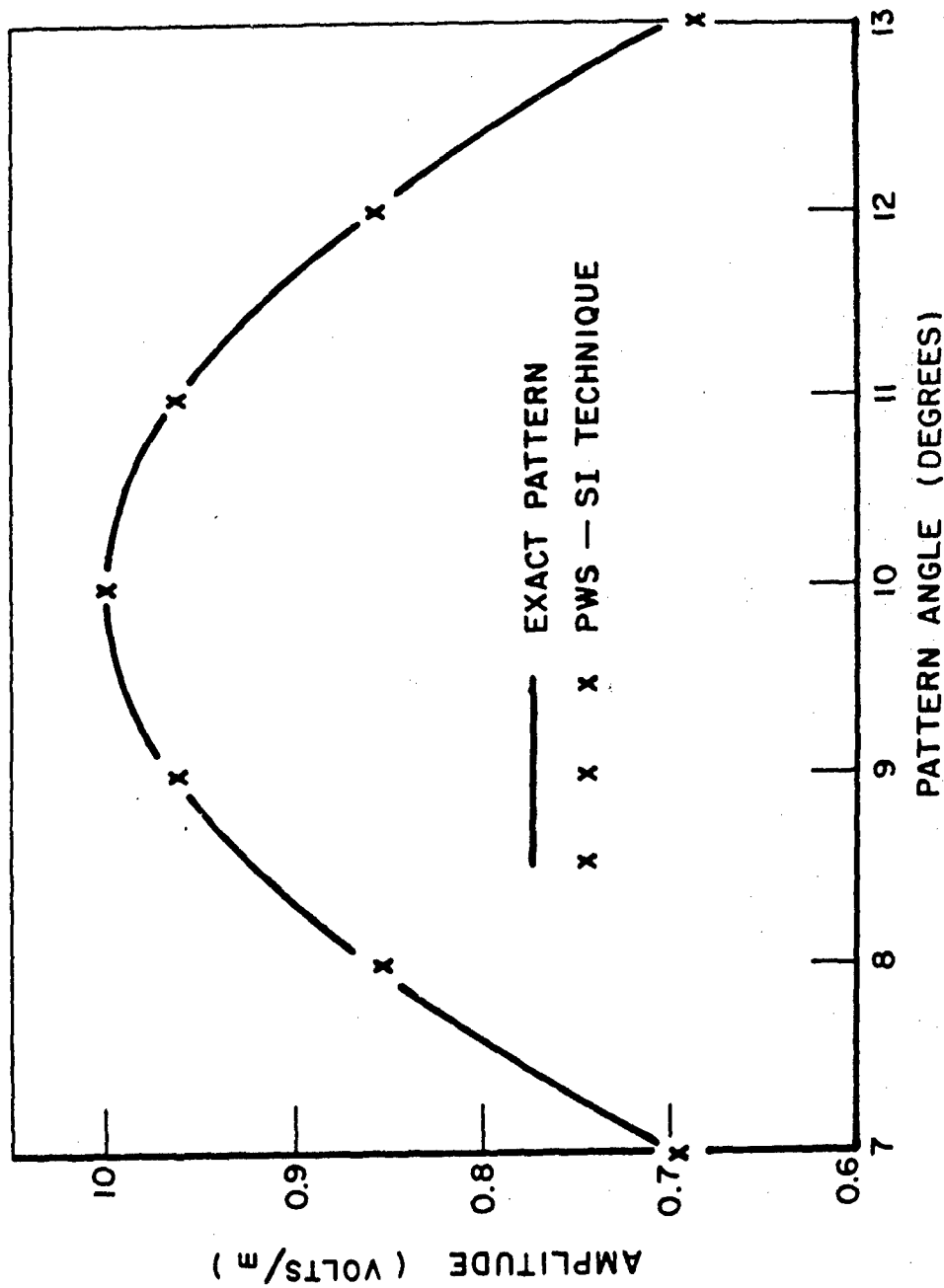


Fig. 7--Far-zone pattern obtained by surface integration technique over an ogive free-space (no radome present) as compared to  $\left| \frac{J_1(x)}{x} \right|$  pattern look angle equals 10°.

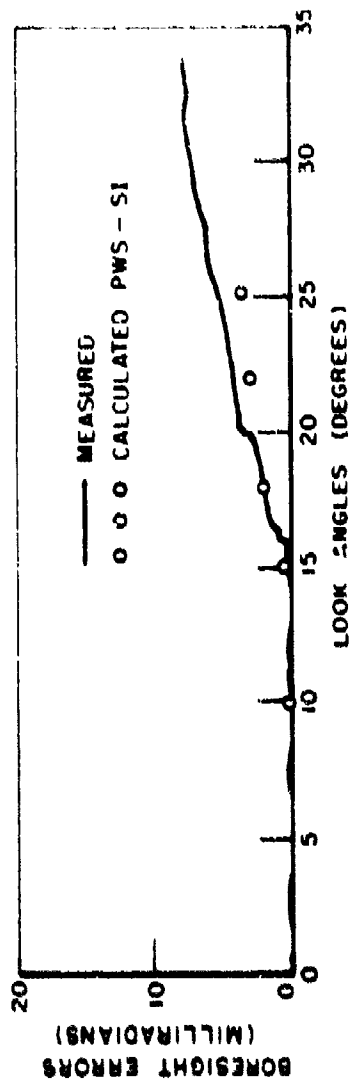


Fig. 8--Calculated and measured boresight error for an ogive radome at design frequency.  
Perpendicular polarization.  
Fineness Ratio 1:1.

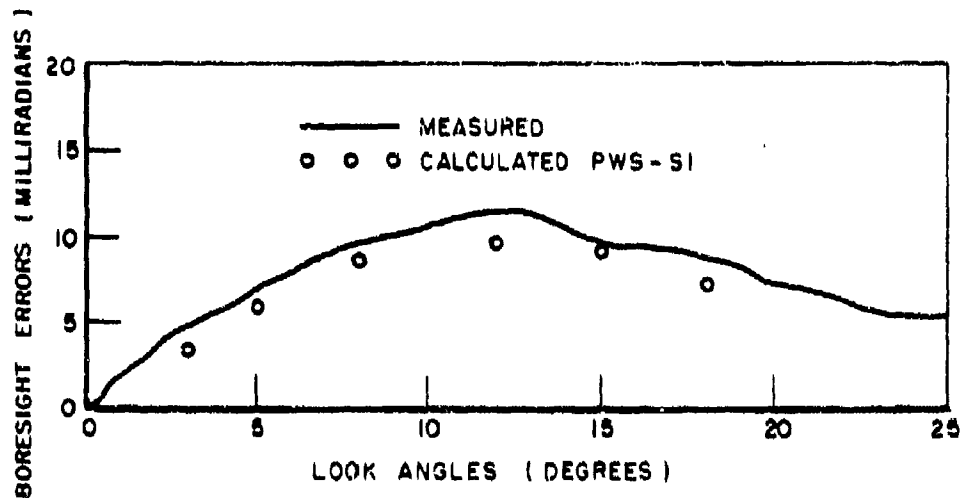


Fig. 9--Calculated and measured boresight error for an ogive radome at design frequency. Perpendicular polarization. Fineness ratio 2:1.

## CHAPTER VI CONCLUSIONS

The research presented here offers a practical method for determining boresight errors in an antenna-radome system. The Plane Wave Spectrum-Surface Integration (PWS-SI) analysis contains the diffraction mechanism necessary to accurately treat practical antenna-radome problems. The Plane Wave Spectrum analysis offers accurate and efficient methods for calculating near-fields of large aperture antennas. Good agreement between theory and measured boresight data is obtained.

It is known that the contribution to boresight error is primarily due to the transmission through the radome of the incident antenna field since only the antenna main lobe region is of interest. Hence, the basic approach for the radome boresight calculation is outlined in steps (a), (b), and (c) as shown in Chapter I. In Chapter V a description of the complete procedure for boresight calculation is presented and an example is worked out to illustrate each step in the procedure. A listing of the PWS-SI computer program is given in Appendix C along with instructions for use of the program.

In the recent developments of antenna-radome systems, considerable attention is being given to the prediction of antenna sidelobes and

backlobes. As an extension of the present study, steps may be included in the PWS-SI technique to account for sidelobe and backlobe contributions as outlined in the following additional steps:

(d) The first order reflected field is calculated, i.e., the fields at 5 due to the antenna incident field at 2 in Fig. 1.

(e) The transmission of the reflected field through the radome is calculated, i.e., from 5 to 6 in Fig. 1.

(f) The total antenna pattern including sidelobe and backlobe contributions may be calculated from the fields on the outer surface of the radome, i.e., the radiation in region 4 or 7 is determined from the fields at 3 and 6.

With steps (d), (e) and (f) added to the PWS-SI technique, it will be capable of accurately calculating antenna pattern distortion, and antenna sidelobe and backlobe behavior for practical three-dimensional antenna-radome combinations. Useful applications include radome systems in the R and D stage as well as operational radomes with boresight or other deficiencies.

APPENDIX A  
 APERTURE INTEGRATION FORMULATION OF A  
 CIRCULAR APERTURE ANTENNA

In this appendix an exact field formulation of an aperture antenna is discussed. In the geometry of Fig. 10, a linear current density polarized in the x-direction flows on the circular surface in the x-y plane. Cylindrical coordinates  $(\rho, \beta, z = 0)$  are used for the current  $M_x(\rho, \beta)$  and the integration point Q on the circular aperture.

For a point of observation P whose position in space is given by spherical coordinates  $(R, \theta, \phi)$  the electric field [16] derived from the vector potential method (see Eqs. (56) and (58)) due to the equivalent magnetic current density  $M_x$  is given by

$$(91) \quad E = - \frac{j}{4\pi} \iint (jk + \frac{1}{r}) M_x \times \hat{r} \frac{e^{-jkr}}{r} da.$$

Similarly, the magnetic field is obtained by applying the duality relations in Table 5 to Eqs. (58) and (59) giving

$$(92) \quad H = - \frac{j}{4\pi\omega\mu} \iint \left\{ \left( -k^2 + \frac{3jk}{r} + \frac{3}{r^2} \right) (M_x \cdot \hat{r}) \hat{r} \right. \\ \left. + k^2 M_x - \frac{M_x}{r} (jk + \frac{1}{r}) \right\} \frac{e^{-jkr}}{r} da.$$

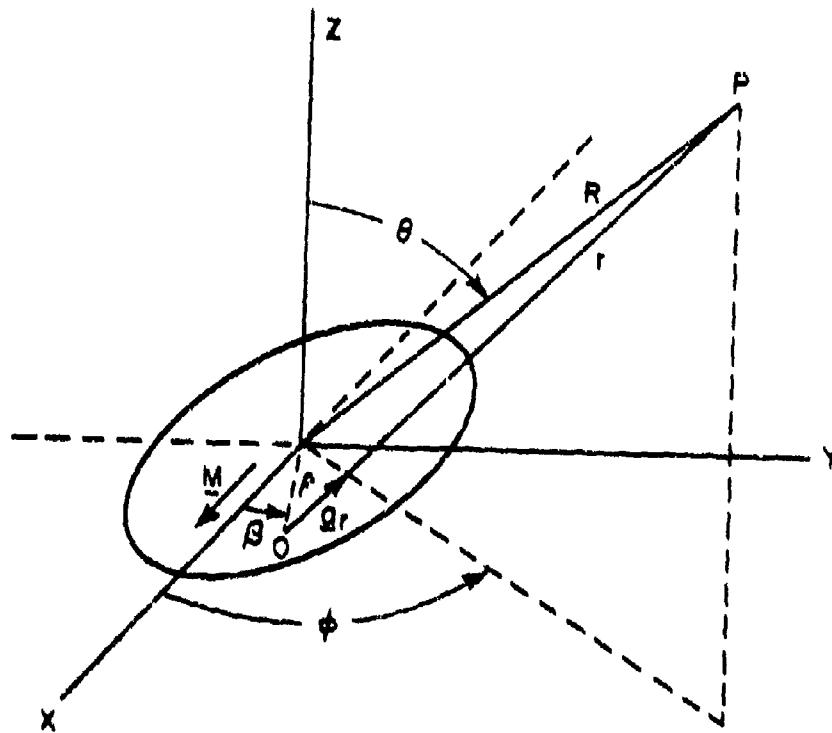


Fig. 10--Aperture and field coordinates.

TABLE 5  
DUAL RELATIONS IN ELECTRIC AND MAGNETIC SYSTEMS

Electric System	Magnetic System
$\vec{J} = \hat{n} \times \vec{H}$ $\vec{E}$ $\vec{H}$ $\epsilon$ $k$	$\vec{M} = \vec{E} \times \hat{n}$ $\vec{H}$ $-\vec{E}$ $\epsilon$ $\mu$ $k$

The distance from Q to P as denoted by r yields

$$(93) \quad r = (R^2 + \rho^2 - 2R\rho \sin\theta \cos(\phi - \beta))^{1/2}.$$

The unit vector r is given by

$$(94) \quad \hat{r} = \hat{x} \left[ \frac{R}{r} \sin\theta \cos\phi - \frac{\rho}{r} \cos(2\phi - \beta) \right]$$

$$+ \hat{y} \left[ \frac{R}{r} \sin\theta \sin\phi - \frac{\rho}{r} \sin\beta \right]$$

$$+ \hat{z} \cos\theta \frac{R}{r}$$

where  $\hat{x}$ ,  $\hat{y}$  and  $\hat{z}$  are the unit vectors and  $\rho$  and  $\beta$  are variables of integration. Hence the electric field of the circular aperture antenna with magnetic current density  $M_x(\rho, \beta)$  polarized in x-direction is given by

$$(95) \quad E_x = 0$$

$$(96) \quad E_y = \frac{1}{4\pi} \int_0^{2\pi} \int_0^a (jk + \frac{1}{r}) M_x(\rho, \beta) \frac{R}{r} \cos \theta \frac{e^{-jkr}}{r} \rho \, d\rho \, d\beta$$

$$(97) \quad E_z = \frac{1}{4\pi} \int_0^{2\pi} \int_0^a (jk + \frac{1}{r}) M_x(\rho, \beta) \left[ \frac{\rho}{r} \sin \beta - \frac{R}{r} \sin \theta \sin \phi \right] \frac{e^{-jkr}}{r} \rho \, d\rho \, d\beta$$

where  $a$  is the radius of the circular aperture. The corresponding magnetic field is given by

$$(98) \quad H_x = -\frac{j}{4\pi\omega\mu} \int_0^{2\pi} \int_0^a \left\{ (-k^2 + \frac{3jk}{r} + \frac{3}{r^2}) \left( \frac{R}{r} \sin \theta \cos \phi - \frac{\rho}{r} \cos(2\phi - \beta) \right)^2 + \left( k^2 - \frac{jk}{r} - \frac{1}{r^2} \right) \right\} M_x(\rho, \beta) \frac{e^{-jkr}}{r} \rho \, d\rho \, d\beta$$

$$(99) \quad H_y = -\frac{j}{4\pi\omega\mu} \int_0^{2\pi} \int_0^a \left( -k^2 + \frac{3jk}{r} + \frac{3}{r^2} \right) \left[ \frac{R}{r} \sin \theta \cos \phi - \frac{\rho}{r} \cos(2\phi - \beta) \right] \left[ \frac{R}{r} \sin \theta \sin \phi - \frac{\rho}{r} \sin \beta \right] M_x(\rho, \beta) \frac{e^{-jkr}}{r} \rho \, d\rho \, d\beta$$

$$(100) \quad H_z = -\frac{j}{4\pi\omega\mu} \int_0^{2\pi} \int_0^a \left(-k^2 + \frac{3jk}{r} + \frac{3}{r}\right)$$

$$\left(\frac{R}{r} \sin\theta \cos\phi - \frac{R}{r} \cos(2\phi - \beta)\right) \cos\theta \frac{R}{r}$$

$$M_x(\rho, \beta) \frac{e^{-jkr}}{r} \rho \, d\rho \, d\beta .$$

The current distribution function  $M_x(\rho, \beta)$  for the uniform case is given by

$$(101) \quad M_x(\rho, \beta) = 2 E_y$$

where  $E_y$  is the aperture electric field polarized in y-direction. Hence in order to compare this aperture integration with the PWS formulation as derived in Chapter II for the unity aperture field, the magnetic current density  $M_x(\rho, \beta)$  equals to 2.

The y-component of the electric field of a uniform circular aperture antenna using the aperture integration method Eq. (96) is compared in Chapter II with the PWS formulation Eq. (15) on a plane surface  $2\lambda$ ,  $10\lambda$ ,  $20\lambda$  and  $40\lambda$  away from the aperture respectively. As mentioned in Chapter II, excellent agreements between the two methods have been obtained.

Comparisons are also made for the near fields of a  $10\lambda$  diameter uniform circular aperture antenna vs. a two dimensional  $10\lambda$  strip antenna with uniform illumination. Both phase and magnitude distributions are compared on a plane surface placed  $2\lambda$ ,  $10\lambda$ ,  $20\lambda$  and  $40\lambda$  from the aperture antenna as shown in Figs. 11-14 respectively. As seen in Fig. 11 the fields at  $2\lambda$  away from a circular aperture antenna are almost the same as a two-dimensional strip antenna. However the finiteness of the circular aperture antenna becomes apparent as the distance away from the aperture is increased. Thus it is seen from Figs. 12-14 that the main lobe of the circular aperture antenna is shaping up faster than that of the two-dimensional strip antenna as the distance from the aperture antennas increases.

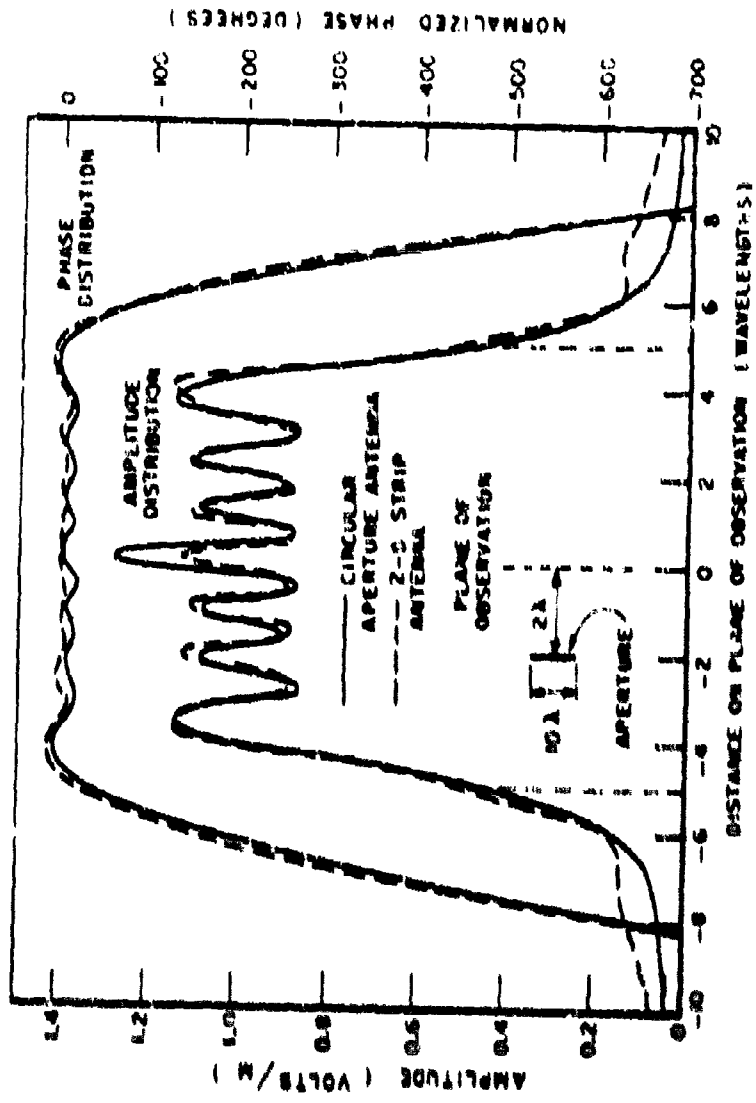


Fig. 11--Comparison of near fields of circular aperture antenna vs. 2-D strip antenna. (TE Polarization).

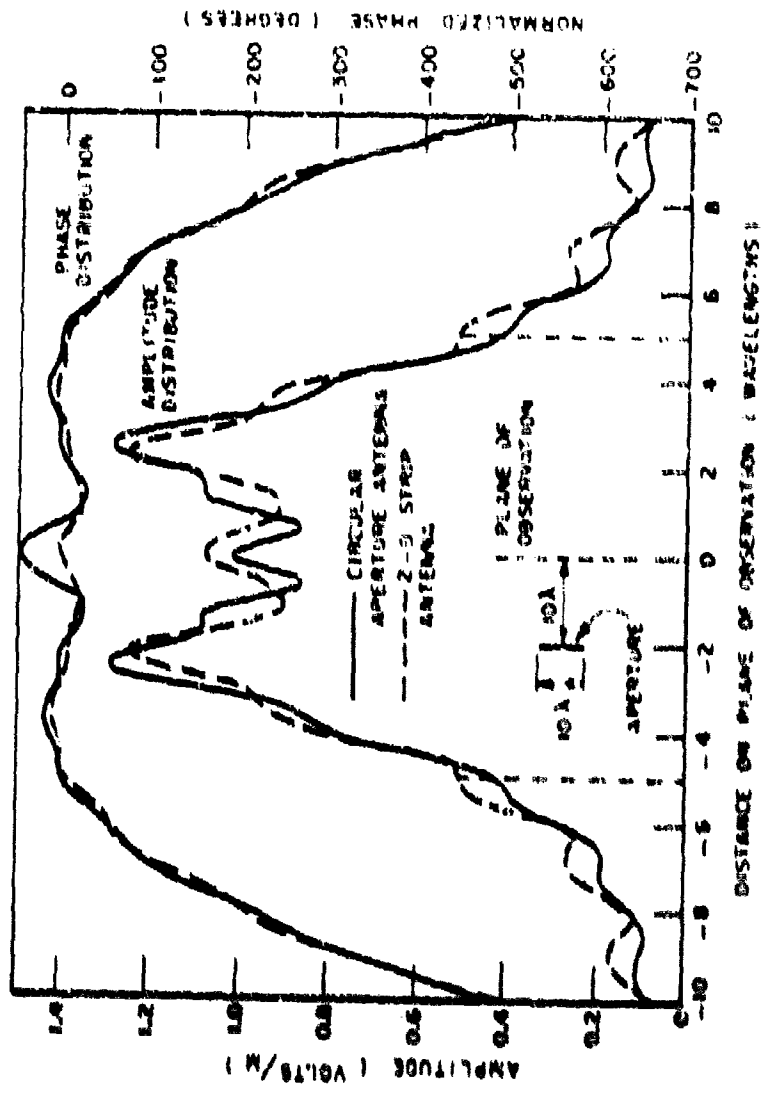


Fig. 12--Comparison of near fields of circular aperture antenna vs. 2-3 strip antenna. (TE polarization).

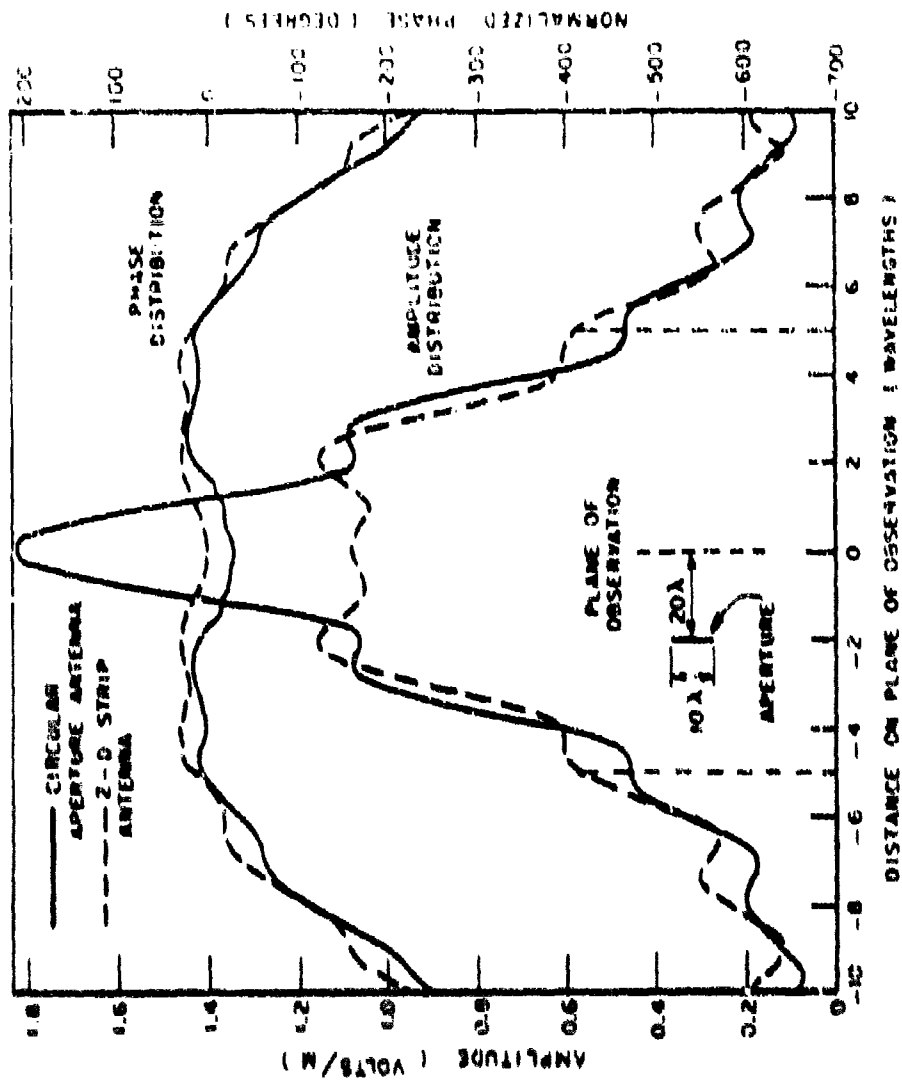


Fig. 13--Comparison of near fields of circular aperture antenna vs. 2-D strip antenna. (TE Polarization).

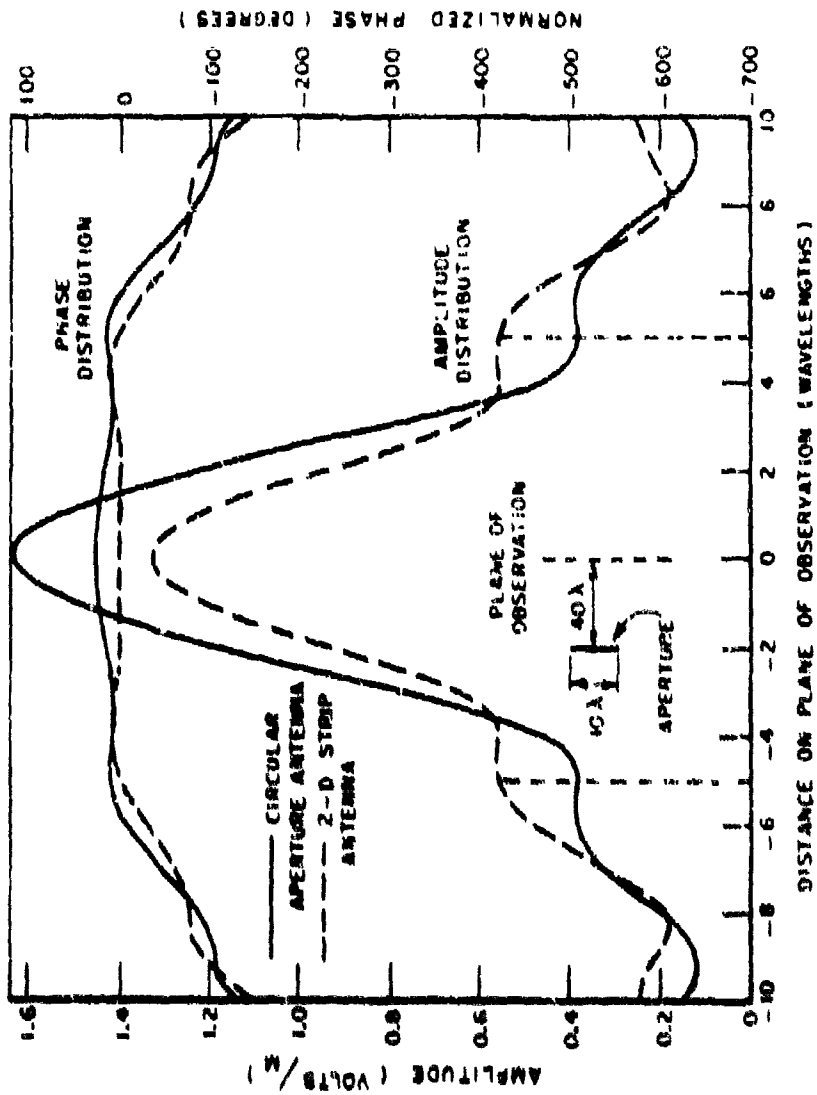


Fig. 14--Comparison of rear fields of circular aperture antenna vs. 2-D strip antenna. (TE Polarization).

APPENDIX B  
APPLICATION OF PLANE WAVE SPECTRUM REPRESENTATION  
TO THE TRANSMITTED FIELD ON RADOME OUTER SURFACE

Virtually all radome analyses treat the transmission through a point on the radome the same as the transmission of a local plane wave through a planar sheet tangential to the point on the curved radome surface. The PWS formulation will now be used to check the local plane wave assumption.

For simplicity a two-dimensional model is considered as shown in Fig. 15 for an aperture of width  $a$  with a uniform  $y$ -polarized electric field. The antenna near field at point  $(x, z)$  in terms of the angular spectrum of plane waves[11] is given by

$$(102) \quad E_y(x, z) = \frac{1}{\lambda} \int_{-\frac{a}{2}}^{\frac{a}{2}} \frac{2}{ks} \sin \frac{ksa}{2} e^{-jk(sx + \sqrt{1-s^2} z)} ds.$$

Consequently, the transmitted field on the outer surface of the radome can be derived by a weighting function  $W(\theta_1)$  which represents the effect of the radome on each plane wave in the spectrum. This gives

$$(103) \quad E_y(x, z) = \frac{1}{\lambda} \int_{-1}^1 W(\theta_1) F(s) e^{-jk(sx + \sqrt{1-s^2} z)} ds.$$

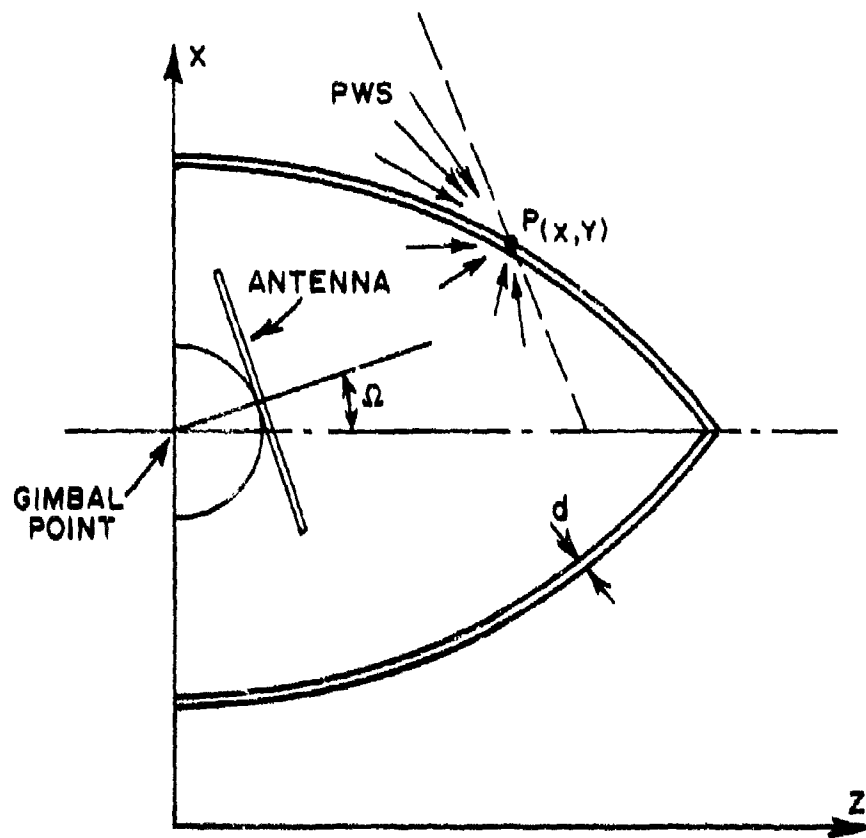


Fig. 15--Radome geometry.

The weighting function corresponds to the plane wave transmission coefficient in the portion of the spectrum for which the plane waves are incident from inside the radome. For incidence outside the radome the weighting function is given by the sum of the incident and reflected waves, thus  $W(\theta_i) = 1 + r(\theta_i)$  for perpendicular polarization.

The transmitted electric field  $E_y(x,z)$  on the outer surface of a 2-D half-wave-length wall ogive radome with low loss homogeneous material is shown in Fig. 16 using the above analysis. The  $10\lambda$  antenna is situated at a look angle of  $20^\circ$  as shown in Fig. 15. The tip of radome is at  $z = 24.48\lambda$ . Results calculated by the Wedge Diffraction formulation[4] are also shown for comparison. It is seen from Fig. 16 that both magnitude and phase of  $E_y(x,z)$  check well using the above two formulations for  $z > 12\lambda$ . Hence the local plane wave approximation used in the wedge diffraction analysis is accurate in that region. However for  $z \leq 12\lambda$ , small deviations are observed between the two techniques. It is concluded that the local plane wave approximation used in conventional radome analyses is not as accurate as the PWS formulation in the close near field region.

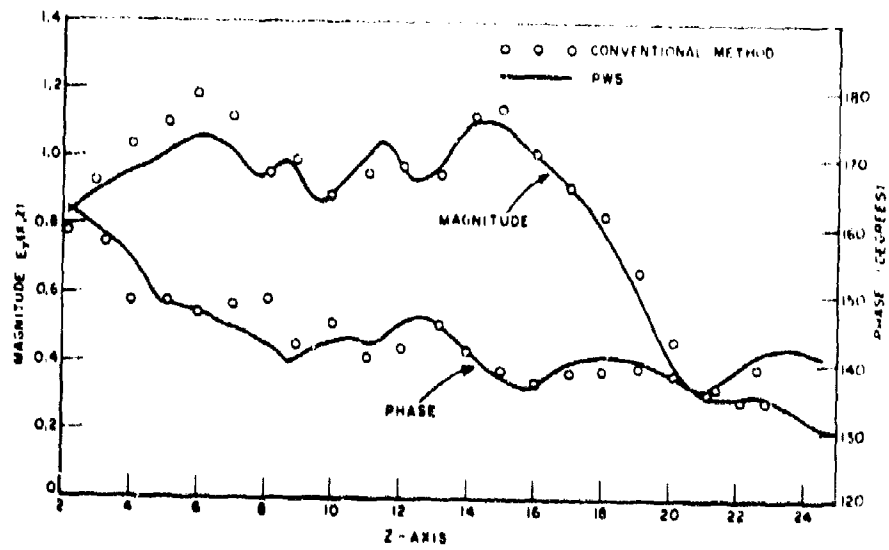


Fig. 16--Transmitted field on the outer radome surface using PWS and conventional formulations.

APPENDIX C  
INSTRUCTION FOR USE OF COMPUTER PROGRAM

A complete listing of the PWS-SI computer program using Fortran IV programming language is given in this appendix for radome boresight analysis. The input data for the calculation of boresight error of a typical one layer fiberglass ogive radome having a 1:1 fineness ratio is listed at the end of the computer program on page 81. There are seven input cards which are explained in the following for this calculation.

1. Number of layers.
2. Dielectric constant, wall thickness and loss tangent.
3. Number of geometry sections used to define the radome shape.
4. Coefficients of a general second degree equation which defines the radome geometry, i.e.,

$$aZ^2 + bXZ + cX^2 + dZ + eX + f = 0.$$

- 5,6,7. Radius of the aperture antenna, look angle and the distance from the gimbal point to the aperture antenna.

Three boresight error calculations are obtained at look angles 15°, 18° and 22° respectively. The output of this program also contains information for a check of free space pattern as discussed in Chapter V.

```

// 15000,CLASS#0
//FORT FXFC PGM=IFYFORT,PARM='MAP,RCN',TIME=(0,30)
//SYSPRINT DD SYSOUT=C,DCB=(RECFM=DA,LRI CL=120,
// BLKSIZE=600),SPACE=(CYL,(1,1),RLSE)
//SYSLIN DD UNIT=SYSDA,DSNAME=CALLDADSET,DISP=(MOD,PASS),
// SPACE=(CYL,(1,1)),DCB=(RECFM=FB,LRI CL=40,BLKSIZE=600)
//SYSIN DD *
C   THREE DIMENSIONAL ANTENNA-RADOME BORESIGHT ANALYSIS
C   PWS AND SURFACE INTEGRATION METHODS FOR RADOME BORESIGHT ANALYSIS
C   THIS IS A PROGRAM FOR EVALUATING THE FIELDS IN RADOME PROBLEMS.
COMPLEX AHZ,ATF,APH, AME,ATH,SHX,SHY,SHZ
COMPLEX SEX,SFY,SFZ,SYR,SYRP
DIMENSION THETA(3),THETR(3),AE(3)
COMPLEX ATT,STT,AFX
COMPLEX SXH(30,45),SYH(30,45),SZH(30,45)
COMPLEX EHX(30,45),FHY(30,45),EHZ(30,45)
COMPLEX ERX(30,45),ERY(30,45),ERZ(30,45)
COMPLEX SRX(30,45),SRY(30,45),SRZ(30,45)
COMPLEX EY,EZ,HX,HY,HZ,OR,AEY,AEZ,AHZ,AHX,AHY
COMPLEX CHX,CHY,CHZ,OY
102 DIMENSION AA(5),BB(5),CC(5),DD(5),EE(5),FF(5),DELT(5)
FORMAT(20X,7H THETA=,F10.5)
COMPLEX EXJP,FYR,FYRP
DIMENSION UXR(30,45),UZR(30,45),PN(30,45)
COMMON Z,PHI,P,TP,TPA
DIMENSION X(25),W(25)
COMMON/XX/ X,W
X(01)=0.072380170962869262033
X(02)=0.097004699209462698030
X(03)=0.16122356068991718056
X(04)=0.2247637903946899061225
X(05)=0.287362487455655576736
X(06)=0.348755886792160738160
X(07)=0.408686661990716729916
X(08)=0.466902904750558404545
X(09)=0.523160974722233033678
X(10)=0.577224726083972703518
X(11)=0.628867396776513623995
X(12)=0.677872379632663905212
X(13)=0.7240341309238146654674
X(14)=0.767159022515740339254
X(15)=0.807066206074442627083
X(16)=0.843588261624393530711
X(17)=0.876572020274247885906
X(18)=0.905879136715569672822
X(19)=0.931386690706554333114
X(20)=0.952987703160430860723
X(21)=0.970591592546247250461
X(22)=0.984124583722826857745
X(23)=0.993530172266350757548
X(24)=0.998771007252426118601
W(01)=0.064737696812683922503
W(02)=0.064466164435950082207
W(03)=0.063524238584648186624
W(04)=0.063114192786254025657
W(05)=0.062039423159892663904
W(06)=0.060704439165893880053
W(07)=0.059114839658395635746
W(08)=0.057277292100403215705
W(09)=0.055199503699984162868
W(10)=0.052890189485193667096

```

```

* 100703
100704
* 100705
100706
100707

```

```

W(11)=0.050459035553856674958
W(12)=0.047616658492490474826
W(13)=0.044674560456694280419
W(14)=0.041845082963466749214
W(15)=0.038241351065830706317
W(16)=0.034777222566770438893
W(17)=0.031167227832798088902
W(18)=0.027426509708156968200
W(19)=0.023570760139326479141
W(20)=0.01961616045735527814
W(21)=0.015579315722963860728
W(22)=0.011477236879236539490
W(23)=0.007327553901276262102
W(24)=0.003153346052305838633
OR # X0.,0.<
OY # X0.,-1.<
OX # 0.
WRITE #6,4<
4 FORMAT #1X,63HTHIS IS A PROGRAM FOR EVALUATING THE FIELDS IN RADOM
2E PROBLEMS.<
DIMENSION DC(10)
REAL LD(10),LT(10)
COMPLEX TPAR,TPFR
READ(5,25) NK,(DC(I),LD(I),LT(I),I=1,NK)
25 FORMAT(110/3F10.4)
IPE=0
IPI=1
READ(5,100)N,(AL(I),BB(I),CC(I),DD(I),EE(I),FF(I),DELT(I),I=1,N)
100 FORMAT(15/7F10.5)
DO 999 ICA=1,3
READ(5,101) ALFN,OMEGA,R3
101 FORMAT(7F10.5)
PI=3.14159265
TP=2.*PI
TPA=TP*ALFN
DR=PI/180.
RR=1./DR
(OMR=OMEGA*DR
COM=COS(OMR)
SOM=SIN(OMR)
RL=0.
RU=1.
NG=4
C RADOME GEOMETRY
COUT=COM
SOUT=SOM
EYK=(0.,0.)
SYK=(0.,0.)
DO 300 J=1,N
A=AA(J)
B=BB(J)
C=CC(J)
D=DD(J)
E=EE(J)
F=FF(J)
RRC=SQRT(D*D+E*F-4.*F)/2.
G=SQRT(RRC*RRC-F*E/4.)
THE1=ATAN2(G,E/2.)-0.0001
THE2=0.
JTT=20
FTJT=JTT+1
C DEFINE POINTS ON THE INNER RADOME SURFACE

```

```

      DO 400 JT=1,JTT
      FJT=JT-1
      FJT=FJT+0.5
      ZZ=RKC*SIN(THET1-FJT*(THET1-THET2)/FTJT)
      CALL YC (A,B,C,D,E,F,ZZ,XY)
      NX=36
      IF(XY.LE.2.5) NX=1R
      FX=NX
C     FIND NORMAL VECTOR
      CALL NORM(A,B,C,D,E,ZZ,XY,AZR,AXA,ANORM)
      RR=SQRT(ZZ*ZZ+XY*XY)
      STH=XY/RR
      CTH=ZZ/RR
      NP=NX/2+1
      PHAI=TP/FX
      DO 500 JP=1,NP
      PHAI=TP*2./FX
      IF(JP.EQ.1) PHAI=PHAI/2.
      IF(JP.EQ.NP) PHAI=PHAI/2.
      FJP=JP-1
      PHII=PHAI*FJP
      COSP=COS(PHII)
      SINP=SIN(PHII)
      XX=XY*COSP
      YY=XY*SINP
      AXR=AXA*COSP
      AYR=AXA*SINP
      XA=COSM*XX-SOM*Z7
      YA=YY
      Z=SOM*XX+COSM*ZZ-R3
      IF(Z) 650,650,660
660  AXRA=AXR*COSM-AZR*SOM
      AYRA=AYR
      AZRA=AXR*SOM+AZR*COSM
      P=SQRT(XA*XA+YA*YA)
      PHI=ATAN2(YA,XA)
      COSP=XA/P
      SINP=YA/P
      CALL GAUS(RL,RU,MG,EY,EZ,HX,HY,HZ)
      EY=EY*TPA
      EZ=EZ*QY*SINP*TPA
      HX=-HX*TPA
      HY=-HY*0.5*TPA*CIN(2.*PHI)
      HZ=-HZ*QY*TPA*COSP
      EYPP=ATAN2(AI*AG(EY),REAL(EY))*RD
      CHX # CONJG*HX<
      CHY # CONJG*HY<
      CHZ # CONJG*HZ<
      GX # REAL*FY*CHZ-EZ*CHY<
      GY # REAL*EZ*CHX<
      GZ # REAL*EY*CHX<
      AMP # SQRT*GX*GX*GY*GY*GZ*GZ<
      UX # GX/AMP
      UY # GY/AMP
      UZ # GZ/AMP
      TX=AYRA*UX-AZRA*UY
      TY=AZRA*UX-AXRA*UY
      TZ=AXRA*UY-AYRA*UX
      TT=SQRT(TX*TX+TY*TY+TZ*TZ)*(-1.)
      TX=TX/TT
      TY=TY/TT
      TZ=TZ/TT

```

```

TXX=CIM*TX+SIM*TZ
TZZ=-SOM*TX+CIM*TZ
TNX=TY*AZRA-TZ*AYRA
TNY=TZ*AXRA-TX*AZRA
TNZ=TX*AYRA-TY*AXRA
TN=SQRT(TNX*TNX+TNY*TNY+TNZ*TNZ)
TNX=TNX/TN
TNY=TNY/TN
TNZ=TNZ/TN
PN(JT,JP)=UX*AXRA+UY*AYRA+UZ*AZRA
UTHET=ARCOS(PN(JT,JP))
CALL TPCD(IPR,NK,UTHET,LD,DC,LT,TC,FIPD)
TPER=TC*CEXP(CMPLX(0.,-FIPD*DR))
TC1=TC
FIPD1=FIPD
CALL TPCD(IPR,NK,UTHET,LD,DC,LT,TC,FIPD)
TPAR=TC*CEXP(CMPLX(0.,-FIPD*DR))
TC2=TC
FIPD2=FIPD
ATE=TY*EY+TZ*EZ
ANE=TNY*EY+TNZ*EZ
ATH=TX*HX+TY*HY+TZ*HZ
ANH=TNX*HX+TNY*HY+TNZ*HZ
AEX=ATF*TX*TPER+ANE*TNX*TPAR
AEY=ATE*TY*TPER+ANE*TNY*TPAR
AEZ=ATE*TZ*TPER+ANE*TNZ*TPAR
AHX=ATH*TX*TPAR+ANH*TNX*TPER
AHY=ATH*TY*TPAR+ANH*TNY*TPER
AHZ=ATH*TZ*TPAR+ANH*TNZ*TPER
SEX=ATE*TX+ANE*TNX
SEY=ATE*TY+ANE*TNY
SEZ=ATE*TZ+ANE*TNZ
SHX=ATH*TX+ANH*TNX
SHY=ATH*TY+ANH*TNY
SHZ=ATH*TZ+ANH*TNZ
ERX(JT,JP)=COM*AEX+SOM*AEZ
ERY(JT,JP)=AEY
ERZ(JT,JP)=-SOM*AEX+COM*AEZ
SRX(JT,JP)=COM*SEX+SOM*SEZ
SRY(JT,JP)=SEY
SRZ(JT,JP)=-SOM*SEX+COM*SEZ
EHX(JT,JP)=COM*AHX+SOM*AHZ
EHY(JT,JP)=AHY
EHZ(JT,JP)=COM*AHZ-SOM*AHX
SXH(JT,JP)=COM*SHX+SOM*SHZ
SYH(JT,JP)=SHY
SZH(JT,JP)=COM*SHZ-SOM*SHX
UXR(JT,JP)=COM*UX+SOM*UZ
UZR(JT,JP)=-SOM*UX+COM*UZ
EXJ=RR*TP*(SOOT*STH*COIP+COOT*CTH)
EXJD=EXJ*RD
EXJP=CEXP(CMPLX(0.,EXJ))
EYRP=(-AXR*(SOOT*ERY(JT,JP)+EHZ(JT,JP))+AYR*(SOOT*ERX(JT,JP)+COOT*
1ERZ(JT,JP))+AZR*(EHX(JT,JP)-COOT*ERY(JT,JP)))*EXJP*XY*PHAI
EYR=EYR+EYRP
FYRR=CABS(FYR)
EYRA=ATAN2(AIMAG(EYR),REAL(EYR))*RD
SYRP=(-AXR*(SOOT*SRX(JT,JP)+SZH(JT,JP))+AYR*(SOOT*SRX(JT,JP)+COOT*
1SRZ(JT,JP))+AZR*(SXH(JT,JP)-COOT*SRX(JT,JP)))*EXJP*XY*PHAI
SYR=SYR+SYRP
SYRR=CABS(SYR)
SYRA=ATAN2(AIMAG(SYR),REAL(SYR))*RD

```

```

GO TO 750
650 ERX(JT,JP)=(0.,0.)
    ERY(JT,JP)=(0.,0.)
    ERZ(JT,JP)=(0.,0.)
    SRX(JT,JP)=(0.,0.)
    SRY(JT,JP)=(0.,0.)
    SRZ(JT,JP)=(0.,0.)
    PN(JT,JP)=0.
    UXR(JT,JP)=0.
    UZR(JT,JP)=0.
    EHX(JT,JP)=(0.,0.)
    EHY(JT,JP)=(0.,0.)
    EHZ(JT,JP)=(0.,0.)
    SHX(JT,JP)=(0.,0.)
    SHY(JT,JP)=(0.,0.)
    SHZ(JT,JP)=(0.,0.)
750 CONTINUE
500 CONTINUE
    WRITE(6,6) XX,YY,ZZ,XA,YA,Z
    6 FORMAT(2/1X,20H FIELD POINT : X = ,F5.2,2X,4HY = ,F5.2,2X,4HZ 8 ,
      2F5.2,2X,4HR = ,F5.2,2X,5HTH = ,F5.2,2X,6HPHI = ,F5.2<
68 WRITE(6,88) TX,EY,FYPP,TY,EZ,TZ,HX,AXRA,HY,AYRA,HZ,AZRA
88 FORMAT(2/5X,6HEY = ,7X,4*2X,E15.8</5X,6HEZ = ,7X,3*2X,E15.8</5X,6
  2HHX = ,7X,3*2X,E15.8</5X,6HHY = ,7X,3*2X,E15.8</5X,6HHZ = ,7X,4
  3*2X,E15.8<<
    WRITE(6,105) AEX,AEY,AEZ,AHX,AHY,AHZ
    WRITE(6,105) SEX,SEY,SEZ,SHX,SHY,SHZ
105 FORMAT(2X,12F9.6)
    WRITE(6,57) UX,UY,UZ
    WRITE(6,57) AXR,AYR,AZR
    WRITE(6,57) TX,TY,TZ
    WRITE(6,57) UXR(JT,JP),UY,UZR(JT,JP)
57 FORMAT(2/46H THE DIRECTION OF POYNTING VECTOR IS : UX = ,F10.5,8
  2H UY = ,F10.5,8H UZ = ,F10.5<
    WRITE(6,89) JT,JP,ERX(JT,JP),ERY(JT,JP),ERZ(JT,JP)
    WRITE(6,89) JT,JP,SRX(JT,JP),SRY(JT,JP),SRZ(JT,JP)
89 FORMAT(2/110,6(2X,F12.5))
    WRITE(6,900) FYPP,FYR,FYRR,FYRA,EXJD
    WRITE(6,900) SYRP,SYR,SYRR,SYRA
    WRITE(6,900) PN(JT,JP),UTHET,TC1,FIPD1,TC2,FIPD2
    WRITE(6,900) FYRP,EYR,FYRR,EYRA,THAB
900 FORMAT(7(1X,E14.7))
    WRITE(6,900) SYRP,SYR,SYRR,SYRA
    WRITE(6,1111) JT,JP
1111 FORMAT(2I20)
400 CONTINUE
300 CONTINUE
    THETB=(OMEGA-11.)*DR
    THAB=OMEGA-11.
    DO 350 JLP=2,22
    THAB=THAB+1.
    WRITE(6,102)THAB
    THETB=THETB+DR
    IF(JLP.EQ.12) GO TO 350
    EYR=(0.,0.)
    SYR=(0.,0.)
    SOOT=SIN(THETB)
    COOT=COS(THETB)
    DO 460 JT=1,JT
    FJT=JT-1
    FJT=FJT+0.5
    ZZ=RRC*SIN(THETB-FJT*(THETB-THETC)/FTJT)

```

```

CALL YC (A,B,C,D,F,F,ZZ,XY)
NX=36
IF(XY.LE.2.5) NX=18
FX=NX
PAHI=TP/FX
C FIND NORMAL VECTOR
CALL NORM(A,B,C,D,E,ZZ,XY,AZR,AXA,ANORM)
RR=SQRT(ZZ*ZZ+XY*XY)
STH=XY/RR
CTH=ZZ/RR
NP=NX/2+1
DP=560 JP=1,NP
PHAI=TP*2./FX
IF(JP.EQ.1) PHAI=PHAI/2.
IF(JP.EQ.NP) PHAI=PHAI/2.
FJP=JP-1
PHII=PAHI*FJP
COP=COS(PHII)
SIP=SIN(PHII)
XX=XY*COP
YY=XY*SIP
AXR=AXA*COP
AYR=AXA*SIP
EXJ=RR*TP*(SOOT*STH*COP+COOT*CTH)
EXJD=EXJ*RD
FXJP=EXP(CMPLX(0.,EXJ))
EYRP=(-AXR*(SOOT*ERY(JT,JP)+EHZ(JT,JP))+AYR*(SOOT*ERX(JT,JP)+COOT*
1FRZ(JT,JP))+AZR*(EHX(JT,JP)-COOT*ERY(JT,JP)))*EXJP*XY*PHAI
FYR=EYR+EYRP
EYRR=CAHS(EYR)
FYRA=ATAN2(AIMAG(EYR),REAL(EYR))*RD
SYRP=(-AXR*(SOOT*SRX(JT,JP)+SZH(JT,JP))+AYR*(SOOT*SRX(JT,JP)+COOT*
1SRZ(JT,JP))+AZR*(SXH(JT,JP)-COOT*SRX(JT,JP)))*EXJP*XY*PHAI
SYR=SYR+SYRP
SYRR=CAHS(SYR)
SYRA=ATAN2(AIMAG(SYR),REAL(SYR))*RD
560 CONTINUE
460 CONTINUE
WRITE(6,1111) JT,JP
WRITE(6,900) EYRP,EYR,EYRR,EYRA,EXJD
WRITE(6,900) SYRP,SYR,SYRR,SYRA
350 CONTINUE
554 FORMAT(10X,6HBMAX= ,F10.5,6H BSEM=,F15.8)
KK=0
KL=0
THETA(1)=OMEGA-1.
THETR(1)=THETA(1)*DR
THETA(2)=OMEGA+1.
THETR(2)=THETA(2)*DR
850 KK=KK+1
FYK=(0.,0.)
WRITE(6,102) THETA(KK)
COOT=COS(THETR(KK))
SOOT=SIN(THETR(KK))
DO 462 JT=1,JTT
FJT=JT-1
FJT=FJT+0.5
ZZ=RR* SIN(THETA(1)-FJT*(THETA(1)-THETA(2))/FTJT)
CALL YC (A,B,C,D,E,F,ZZ,XY)
NX=36
IF(XY.LE.2.5) NX=18
FX=NX

```

```

PAHI=TP/FX
CALL NORM(A,B,C,D,F,ZZ,XY,AZR,AXA,ANORM)
RR=SQRT(ZZ*ZZ+XY*XY)
STH=XY/RR
CTH=ZZ/RR
NP=NX/2+1
DO 562 JP=1,NP
PHAI=TP*2./FX
IF(JP.EQ.1) PHAI=PHAI/2.
IF(JP.EQ.NP) PHAI=PHAI/2.
FJP=JP-1
PHII=PAHI*FJP
COP=COS(PHII)
SIP=SIN(PHII)
XX=XY*COP
YY=XY*SIP
AXK=AXA*COP
AYR=AXA*SIP
EXJ=RR*TP*(SOOT*STH*COP+COOT*CTH)
EXJD=EXJ*RD
EXJP=CFXP(CMPLX(0.,EXJ))
EYRP=(-AXR*(SOOT*ERY(JT,JP)+EHZ(JT,JP))+AYR*(SOOT*ERX(JT,JP)+COOT*
1ERZ(JT,JP))+AZR*(FHX(JT,JP)-COOT*ERY(JT,JP)))*EXJP*XY*PHAI
EYR=EYR+EYRP
EYRR=CABS(EYR)
EYRA=ATAN2(AIMAG(EYR),REAL(EYR))*RD
562 CONTINUE
462 CONTINUE
WRITE(6,900) EYRP,EYR,EYRR,EYRA,EXJD
AE(KK)=EYRR
IF(KK.FQ.1.AND.KL.FQ.0) GO TO 850
IF(KL.FQ.11) GO TO 852
KL=KL+1
IF(AE(1)-AE(2)) 851,852,853
853 THETA(2)=(THETA(1)+THETA(2))/2.
THLTR(2)=THETA(2)*DR
KK=1
GO TO 850
851 THETA(1)=(THETA(1)+THETA(2))/2.
THETR(1)=THETA(1)*DR
KK=0
GO TO 850
852 BMAX=(THETA(1)+THETA(2))/2.
BSEM=(BMAX-OMEGA)*DR*1000.
WRITE(6,554) BMAX,BSEM
960 CONTINUE
999 CONTINUE
STOP
END
SUBROUTINE GAUS*RL,RU,M,AXEY,AXEZ,AXHX,AXHY,AXHZ<
COMPLEX SUMX,SUMY,SUMZ,SUMV,SUMW,GEY,GEZ,GHX,GHY,GHZ,AXEY,AXEZ,AX
2HX,AXHY,AXHZ,XEY,XEZ,AXH,AXHY,AXZ
COMMON/XX/ X,W
DIMENSION X(25),W(25)
SUMV # %0.,0.<
SUMW # %0.,0.<
SUMX # %0.,0.<
SUMY # %0.,0.<
SUMZ # %0.,0.<
EM#M
HI#%RU-RL</EM
AO#RL

```

```

H#H1*.5
DO 10 M1#1,M
A1#A0GH
DO 20 I=1,24
H2#H*X#1<
DAH # A1GH2
DAX # A1-H2
CALL FINTGD %DAH,GEY,GEZ,GPX,GHY,GHZ<
CALL FINTGD %DAX,XEY,XFZ,XXH,XHY,XHZ<
SUMV # SUMVEW%I<%%GEY&XEY<
SUMW # SUMWEW%I<%%GEZ&XEZ<
SUMX # SUMXEW%I<%%GHX&XHX<
SUMY # SUMYEW%I<%%GHY&XHY<
20 SUMZ # SUMZEW%I<%%GHZ&XHZ<
10 A0#A0GH1
AXEY # H*SUMV
AXEZ # H*SUMW
AXHX # H*SUMX
AXHY # H*SUMY
AXHZ # H*SUMZ
RETURN
END
SUBROUTINE FINTGD %Y,FEY,FEZ,FHX,FHY,FHZ<
COMPLEX FAC,FEY,FEZ,FHX,FHY,FHZ
COMMON Z,PHI,P,TP,TPA
SY # SORT%1.-Y*Y<
YS # 1./SY
FAC # CEXP%CMPLX%0.,-TP*SY*Z<<
REX # BESL1%TPA*Y<
VX # TP*Y*P
BEVX0=BESL0(VX)
BEVX1=BESL1(VX)
IF(VX.EQ.0.) GO TO 10
BEVX2=(2.*BEVX1/VX)-BEVX0
GO TO 11
10 BEVX2=0.
11 CONTINUE
FEY=BEVX0*REX*FAC
FEZ=-Y*YS*REX*BEVX1*FAC
RX=(1.-0.5*Y*Y)*BEVX0+(0.5*Y*Y)*COS(2.*PHI)*BEVX2
FHX # YS*REX*RX*FAC
FHY=Y*Y*YS*BEX*BEVX2*FAC
FHZ=-Y*BEX*BEVX1*FAC
RETURN
END
FUNCTION BESL0%X<
%X.GT.0.<
Z#ABS%X<
Y#X/3.
Y2#Y*Y
Y3#Y2*Y
Y4#Y2*Y2
Y5#Y3*Y2
Y6#Y4*Y2
Y8#Y6*Y2
Y10#Y8*Y2
Y12#Y10*Y2
IF%X.GT.3.<GO TO 10
BESL0#1.-2.2499997*Y2&1.2656208*Y4-.3163866*Y6&.0444479*Y8-.003944
24*Y10-.00024846*Y12
GO TO 11
10 CONTINUE

```

```

      F#.79788456-2.00000077/Y<-X.00552740/Y3<-X.00009512/Y3<&X.00137237
      2/Y4<-X.00072805/Y5<&X.00014476/Y6<
      T#X-.78534816-X.04166397/Y<-X.00003954/Y2<&X.00262573/Y3<-X.000541
      225/Y4<-X.00029333/Y5<&X.00013558/Y6<
      BFL10#F#COS#T</SQRT#X<
11  CONTINUE
      RETURN
      END
      FUNCTION BFL1#X<
C    POLYNOMIAL APPROXIMATION X.GT.0.
      Y#X/3.
      Y2#Y*Y
      Y3#Y2*Y
      Y4#Y3*Y
      Y5#Y4*Y
      Y6#Y5*Y
      Y8#Y6*Y2
      Y10#Y8*Y2
      Y12#Y10*Y2
      IF#X.GT.3.<GO TO 10
      BFL#0.5-.56249985*Y2&.21093573*Y4-.03954289*Y6&.00443319*Y8-.0003
      21761#Y10&.00001109*Y12
      BFL1#X#BFL#
      GO TO 11
10  CONTINUE
      F#.79788456&X.00000156/Y<&X.01659667/Y2<&X.00017105/Y3<-X.00249511
      2/Y4<&X.00113653/Y5<-X.00070033/Y6<
      T#X-2.35619449&X.12499612/Y<&X.00005650/Y2<-X.00637879/Y3<&X.00074
      2348/Y4<&X.00079824/Y5<-X.00029166/Y6<
      BFL1#F#COS#T</SQRT#X<
11  CONTINUE
      RETURN
      END
CSUBROUTINE #YC* CALCULATES THE #Y#Y-ORDINATE OF A GENERAL SECOND DEGREE
EQUATION WHEN THE X-ORDINATE IS GIVEN
CINPUT A,B,C,D,E,F ARE CONSTANTS OF THE SECOND DEGREE EQUATION
CINPUT X IS THE X-ORDINATE
COUTPUT Y IS THE Y-ORDINATE
      SUBROUTINE YC #A,B,C,D,E,F,X,Y<
      T1#C
      T2#B#X&E
      T3#A#X#X&D#X&F
      Y#X-T2&SQRT#T2*T2-4.0*T1*T3<</#2.0*T1<
      RETURN
      END
C    NORMAL OF A RADOM
SUBROUTINE NORM#A,B,C,D,E,XR,YR,AXR,AYR,ANORM<
      T1#2.#A#XR&B#YR&D
      T2#2.#C#YR&B#XR&E
      T3#SQRT#T1*T1&T2*T2<
      AXR#T1/T3
      AYR#T2/T3
      ANORM#ATAN2#AYR,AXR<
      RETURN
      END
CSUBROUTINE #TCPD* CALCULATES THE #T#TRANSMISSION #C#COEFFICIENT AND #P#
CPHASE #D#DELAY THRU THE RADOME
CINPUT #P#DETERMINES POLARIZATION IF P#0.0 POLAR IS PERPEND. IF P#1.0
CPOLAR IS PARALLEL,#NK#IS THE#NK#NUMBER OF LAYERS,#T# IS THE ANGLE OF
CINCIDENCE #T#THETA #RADIANS< #D#,#E#,#TD# ARE ARRAYS FOR THICKNESS,
CDIELECTRIC CONSTANT AND LOSS TANGENT OF EACH LAYER
COUTPUT #TC# AND#FIPD# ARE THE TRANSMISSION COEFFICIENT AND INSERTION

```

```

CPHASE DELAY
SUBROUTINE TCRD X P,N,T,D,E,TD,TC,FIPOK
DIMENSION DS10<,EX10<,TDX10<,SRX10<,GX10<,RX10<
PI=3.14159265
RADFG=180./PI
DEGRAD=PI/180.
INTEGER P
N=N*PI
FZNE1<#1.
DDD#0.0
DO 5 I#1,N
5 DDD#DDDED*IC
DD#2.0*PI<COS*TC<DDD
S#SIN*TC<SIN*TC
SR*IC<SORT*E*IC<S<
IFZP<6,6,7
6 RR#XSR*IC<COS*TC<XSR*IC<ECOS*TC<
DO 10 I#1,N
II#IEI
SR*II<#SORT*FX*II<S<
GX<I<#2.0*PI*DX<SR*IC
10 RZ<I<#XSR*II<SR*IC<XSR*II<ESR*II<
GO TO 55
7 RR#XSR*IC<FX<I<#COS*TC<XSR*IC<EX<I<#COS*TC<
DO 11 I#1,N
II#IEI
SR*II<#SORT*FX*II<S<
GX<I<#2.0*PI*DX<SR*IC
11 RZ<I<#XSR*II<SR*II<FX<II<#SR*II<EX<II<#SR*II<
55 A#1.0-XX
DO 15 I#1,N
15 A#A*E1.0-RX<I<
A#1.0/A
W#1.
GG#G*IC/W
CG#COS*GG<
SG#SIN*GG<
AD#PI*FX<I<#TDX<I<#DX<I<#W*SR*II<
X1#CG*%1.-AD<
Y1#-SG*%1.-AD<
X2#-RR*CG*%1.EAD<
Y2#-RR*SG*%1.EAD<
X3#-RR*CG*%1.-AD<
Y3#RR*SG*%1.-AD<
X4#CG*%1.EAD<
Y4#SG*%1.EAD<
DO 35 I#2,NN
IFXI-NN<25,20,50
20 U1#1.0
U2#-R*%N<
U3#-R*%N<
U4#1.0
V1#0.0
V2#0.0
V3#0.0
V4#0.0
GO TO 30
25 II#I-1
AD#PI*EX<I<#TDX<I<#DX<I<#W*SR*II<
GG#G*IC/W
CG#COS*GG<
SG#SIN*GG<

```

```

U1#CG*%1.-AD<
V1#-SG*%1.-AD<
U2#-R%II<*CG*%1.&AD<
V2#-R%II<*SG*%1.&AD<
U3#-R%II<*CG*%1.-AD<
V3#R%II<*SG*%1.-AD<
U4#CG*%1.&AD<
V4#SG*%1.&AD<
30 P1#X1*U1-Y1*V1&X2*U3-Y2*V3
O1#Y1*U1&X1*V1&Y2*U3&X2*V3
P2#X1*U2-Y1*V2&X2*U4-Y2*V4
Q2#Y1*U2&X1*V2&X2*V4&Y2*U4
P3#X3*U1-Y3*V1&X4*U3-Y4*V3
Q3#Y3*U1&X3*V1&X4*V3&Y4*U3
P4#X3*U2-Y3*V2&X4*U4-Y4*V4
Q4#Y3*U2&X3*V2&X4*V4&Y4*U4
X1#P1
X2#P2
X3#P3
X4#P4
Y1#O1
Y2#O2
Y3#O3
35 Y4#O4
RCR#X-X3*X4-Y3*Y4</X4*X4&Y4*Y4<
RCI#X-Y3*X4&X3*Y4</X4*X4&Y4*Y4<
RC2#RCR*RCR&RCI*RCI
RC#SORT*RC2<
TR#X1&X2*RCR-Y2*RCI<*A
TI#Y1&Y2*RCR&X2*RCI<*A
TC2#TR*TR&TI*TI
TC#SORT*TC2<
IF#TR.EQ.O..AND.TI.EQ.O.<TI#TI&.0000001
XX#ATAN2*TI,TR<
FIPD#-RADEG*%XX&DD/W<
IF#FIPD.LT.O.<FIPD#FIPD&360.
50 RETURN
END

```

```

/*
//LKED EXEC PGM=IEVL,PARM='LIST,XREF',TIME=(0,10)
//SYSPRINT DD SYSOUT=C
//SYSLIB DD DSN=SYS1.FORTLIB,DISP=SHR
//SYSLIN DD DSN=SYS2.FORTSSP,DISP=SHR
//SYSLIN DD DSN=EEIDANSET,DISP=(OLD,DELETE),DCB=(BLKSIZE=400)
//SYSLMOD DD DSN=EEGOSSET(00),DISP=(MOD,PASS),
// UNIT=SYSDA,DCB=(RECFM=U,BLKSIZE=7794),SPACE=(CYL,(1,1,1))
//SYSUT1 DD UNIT=SYSDA,SPACE=(CYL,(2,2))
//GD EXEC PGM=*.LKED.SYSLMOD,TIME=9,REGION=500K P
//FT06F001 DD SYSOUT=C,DCB=(RECFM=FBA,LRECL=133,
// BLKSIZE=665),SPACE=(CYL,(1,1),RLSE)
//SYSUDUMP DD SYSOUT=P,DCB=(RECFM=VBA,LRECL=125,BLKSIZE=1629),
// SPACE=(CYL,(2,2))
//FT07F001 DD SYSOUT=B,SPACE=(CYL,(1,1))
//FT05F001 DD *

```

201601  
201602  
201603  
201604  
201605  
201606  
\* 201607  
201608  
201609  
\* 201611  
201612  
\* 201613  
201614  
201615  
201616

4.2	1	.26766	.0005			
1.	0.	1.	0.	17.0621	-164.9347	
5.15	15.	2.1572				
5.15	18.	2.1572				
5.15	22.	2.1572				

\*

## REFERENCES

1. "IEEE Standard Definitions of Terms For Antennas," IEEE Trans. Antennas and Propagation, Vol. AP-17, pp. 264-269.
2. Kilcoyne, N. R., "A Two-Dimensional Ray-Tracing Method for the Calculation of Radome Boresight Error and Antenna Pattern Distortion," Report 2767-2, 2 October 1969, ElectroScience Laboratory, The Ohio State University Research Foundation prepared under Contract N00019-69-C-0325 for Naval Air Systems Command, Washington, D. C.
3. Tricoles, G., "Radiation Patterns and Boresight Error of a Microwave Antenna Enclosed in an Axially Symmetric Dielectric Shell," J. Opt. Soc. Am., 54, No. 9, September 1964, pp. 1094-1101.
4. Clark, D. E., Rudduck, R. C. and Wu, D. C. F., "Two Dimensional Radome Analysis by a Surface Integration Technique," Report 2767-5, 26 February 1970, ElectroScience Laboratory, The Ohio State University Research Foundation; prepared under Contract N00019-69-C-0325, for Naval Air Systems Command, Washington, D. C.
5. Paris, D. T., "Computer-Aided Radome Analysis," IEEE Trans. Antennas and Propagation, Vol. AP-18, January 1970, pp. 7-15.

6. Richmond, J. H., "Calculation of Transmission and Surface-Wave Data for Plane Multilayers and Inhomogeneous Plane Layers," Report 1751-2, 31 October 1963, ElectroScience Laboratory, The Ohio State University Research Foundation; prepared under Contract AF33(615)-1081, for Air Force Avionics Laboratory, Wright-Patterson Air Force Base, Ohio.
7. Intihar, M. R., "Antenna Near Field Evaluation by Plane Wave Spectrum," Master Thesis, Department of Electrical Engineering, The Ohio State University, Columbus, Ohio, September 1970.
8. Booker, H. G. and Clemow, P. C., "The Concept of an Angular Spectrum of Plane Waves and Its Relation to that of Polar Diagram and Aperture Distribution," Proceedings IEE, (1950), 97, Part 111, pp. 11-17.
9. Ekan Lalor, "Conditions for the Validity of the Angular Spectrum of Plane Waves," J. Opt. Soc. Am., Vol. 58, No. 9, September 1968, pp. 1236-1237.
10. Harrington, R. F., Time Harmonic Electromagnetic Fields, McGraw-Hill Book Co., Inc., New York, 1961, pp. 103-116.
11. Wu, D. C. F., and Rudduck, R. C., "Application of Plane Wave Spectrum Representation to Radome Analysis," Proceedings of the Tenth Symposium on Electromagnetic Windows, Georgia Institute of Technology, Atlanta, Georgia, July 1970, pp. 46-50.
12. Walter, C. H., Traveling Wave Antennas, McGraw-Hill Book Co., Inc., New York, 1968, pp. 18-21.

13. Paris, D. T., "Digital Computer Analysis of Aperture Antennas," IEEE Transactions on Antennas and Propagation, Vol. AP-16, No. 2, March 1968, pp. 262-264.
14. Silver, S., Microwave Antenna Theory and Design, McGraw Hill Book Co., Inc., New York, 1949, pp. 84-90.
15. Personal communication from W. Beamer, U. S. Naval Air Development Center, Johnsville, Warminster, Pennsylvania.
16. Hansen, R.C. and Bailin, L.L., "A New Method of Near Field Analysis," IRE Trans. AP-7, pp. S458-S467, December 1959.

14. KEY WORDS	LINK A		LINK B		LINK C	
	ROLE	WT	ROLE	WT	ROLE	WT
Radomes Antennas						

**INSTRUCTIONS**

1. **ORIGINATING ACTIVITY:** Enter the name and address of the contractor, subcontractor, grantee, Department of Defense activity or other organization (*corporate author*) issuing the report.
  - 2a. **REPORT SECURITY CLASSIFICATION:** Enter the overall security classification of the report. Indicate whether "Restricted Data" is included. Marking is to be in accordance with appropriate security regulations.
  - 2b. **GROUP:** Automatic downgrading is specified in DoD Directive 5200.10 and Armed Forces Industrial Manual. Enter the group number. Also, when applicable, show that optional markings have been used for Group 3 and Group 4 as authorized.
  3. **REPORT TITLE:** Enter the complete report title in all capital letters. Titles in all cases should be unclassified. If a meaningful title cannot be selected without classification, show title classification in all capitals in parenthesis immediately following the title.
  4. **DESCRIPTIVE NOTES:** If appropriate, enter the type of report, e.g., interim, progress, summary, annual, or final. Give the inclusive dates when a specific reporting period is covered.
  5. **AUTHOR(S):** Enter the name(s) of author(s) as shown on or in the report. Enter last name, first name, middle initial. If military, show rank and branch of service. The name of the principal author is an absolute minimum requirement.
  6. **REPORT DATE:** Enter the date of the report as day, month, year, or month, year. If more than one date appears on the report, use date of publication.
  - 7a. **TOTAL NUMBER OF PAGES:** The total page count should follow normal pagination procedures, i.e., enter the number of pages containing information.
  - 7b. **NUMBER OF REFERENCES:** Enter the total number of references cited in the report.
  - 8a. **CONTRACT OR GRANT NUMBER:** If appropriate, enter the applicable number of the contract or grant under which the report was written.
  - 8b, 8c, & 8d. **PROJECT NUMBER:** Enter the appropriate military department identification, such as project number, subproject number, system numbers, task number, etc.
  - 9a. **ORIGINATOR'S REPORT NUMBER(S):** Enter the official report number by which the document will be identified and controlled by the originating activity. This number must be unique to this report.
  - 9b. **OTHER REPORT NUMBER(S):** If the report has been assigned any other report numbers (*either by the originator or by the sponsor*), also enter this number(s).
  10. **AVAILABILITY/LIMITATION NOTICES:** Enter any limitations on further dissemination of the report, other than those imposed by security classification, using standard statements such as:
    - (1) "Qualified requesters may obtain copies of this report from DDC."
    - (2) "Foreign announcement and dissemination of this report by DDC is not authorized."
    - (3) "U. S. Government agencies may obtain copies of this report directly from DDC. Other qualified DDC users shall request through \_\_\_\_\_."
    - (4) "U. S. military agencies may obtain copies of this report directly from DDC. Other qualified users shall request through \_\_\_\_\_."
    - (5) "All distribution of this report is controlled. Qualified DDC users shall request through \_\_\_\_\_."
- If the report has been furnished to the Office of Technical Services, Department of Commerce, for sale to the public, indicate this fact and enter the price, if known.
11. **SUPPLEMENTARY NOTES:** Use for additional explanatory notes.
  12. **SPONSORING MILITARY ACTIVITY:** Enter the name of the departmental project office or laboratory sponsoring (*paying for*) the research and development. Include address.
  13. **ABSTRACT:** Enter an abstract giving a brief and factual summary of the document indicative of the report, even though it may also appear elsewhere in the body of the technical report. If additional space is required, a continuation sheet shall be attached.
 

It is highly desirable that the abstract of classified reports be unclassified. Each paragraph of the abstract shall end with an indication of the military security classification of the information in the paragraph, represented as (TS), (S), (C), or (U).

There is no limitation on the length of the abstract. However, the suggested length is from 150 to 225 words.
  14. **KEY WORDS:** Key words are technically meaningful terms or short phrases that characterize a report and may be used as index entries for cataloging the report. Key words must be selected so that no security classification is required. Identifiers, such as equipment model designation, trade name, military project code name, geographic location, may be used as key words but will be followed by an indication of technical context. The assignment of links, rules, and weights is optional.

14. KEY WORDS	LINK A		LINK B		LINK C	
	ROLE	WT	ROLE	WT	ROLE	WT
Radomes Antennas						

INSTRUCTIONS

1. **ORIGINATING ACTIVITY:** Enter the name and address of the contractor, subcontractor, grantor, Department of Defense activity or other organization (*corporate author*) issuing the report.
- 2a. **REPORT SECURITY CLASSIFICATION:** Enter the overall security classification of the report. Indicate whether "Restricted Data" is included. Marking is to be in accordance with appropriate security regulations.
- 2b. **GROUP:** Automatic downgrading is specified in DoD Directive 5200.10 and Armed Forces Industrial Manual. Enter the group number. Also, when applicable, show that optional markings have been used for Group 3 and Group 4 as authorized.
3. **REPORT TITLE:** Enter the complete report title in all capital letters. Titles in all cases should be unclassified. If a meaningful title cannot be selected without classification, show title classification in all capitals in parentheses immediately following the title.
4. **DESCRIPTIVE NOTES:** If appropriate, enter the type of report, e.g., interim, progress, summary, annual, or final. Give the inclusive dates when a specific reporting period is covered.
5. **AUTHOR(S):** Enter the name(s) of author(s) as shown on or in the report. Enter last name, first name, middle initial. If military, show rank and branch of service. The name of the principal author is an absolute minimum requirement.
6. **REPORT DATE:** Enter the date of the report as day, month, year, or month, year. If more than one date appears on the report, use date of publication.
- 7a. **TOTAL NUMBER OF PAGES:** The total page count should follow normal pagination procedures, i.e., enter the number of pages containing information.
- 7b. **NUMBER OF REFERENCES:** Enter the total number of references cited in the report.
- 8a. **CONTRACT OR GRANT NUMBER:** If appropriate, enter the applicable number of the contract or grant under which the report was written.
- 8b, 8c, & 8d. **PROJECT NUMBER:** Enter the appropriate military department identification, such as project number, subproject number, system numbers, task number, etc.
- 9a. **ORIGINATOR'S REPORT NUMBER(S):** Enter the official report number by which the document will be identified and controlled by the originating activity. This number must be unique to this report.
- 9b. **OTHER REPORT NUMBER(S):** If the report has been assigned any other report numbers (*either by the originator or by the sponsor*), also enter this number(s).

10. **AVAILABILITY/LIMITATION NOTICES:** Enter any limitations on further dissemination of the report, other than those imposed by security classification, using standard statements such as:

- (1) "Qualified requesters may obtain copies of this report from DDC."
- (2) "Foreign announcement and dissemination of this report by DDC is not authorized."
- (3) "U. S. Government agencies may obtain copies of this report directly from DDC. Other qualified DDC users shall request through \_\_\_\_\_."
- (4) "U. S. military agencies may obtain copies of this report directly from DDC. Other qualified users shall request through \_\_\_\_\_."
- (5) "All distribution of this report is controlled. Qualified DDC users shall request through \_\_\_\_\_."

If the report has been furnished to the Office of Technical Services, Department of Commerce, for sale to the public, indicate this fact and enter the price, if known.

11. **SUPPLEMENTARY NOTES:** Use for additional explanatory notes.

12. **SPONSORING MILITARY ACTIVITY:** Enter the name of the departmental project office or laboratory sponsoring (*paying for*) the research and development. Include address.

13. **ABSTRACT:** Enter an abstract giving a brief and factual summary of the document indicative of the report, even though it may also appear elsewhere in the body of the technical report. If additional space is required, a continuation sheet shall be attached.

It is highly desirable that the abstract of classified reports be unclassified. Each paragraph of the abstract shall end with an indication of the military security classification of the information in the paragraph, represented as (TS), (S), (C), or (U).

There is no limitation on the length of the abstract. However, the suggested length is from 150 to 325 words.

14. **KEY WORDS:** Key words are technically meaningful terms or short phrases that characterize a report and may be used as index entries for cataloging the report. Key words must be selected so that no security classification is required. Identifiers, such as equipment model designation, trade name, military project code name, geographic location, may be used as key words but will be followed by an indication of technical context. The assignment of links, rules, and weights is optional.